Department of Applied Physics

Thermal transport in mesoscopic devices

Tomi Ruokola

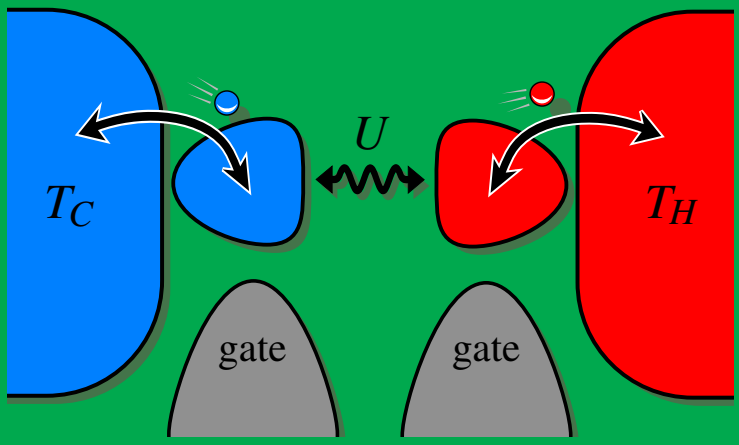

Aalto University

DOCTORAL DISSERTATIONS

Aalto University publication series
DOCTORAL DISSERTATIONS 96/2012

Thermal transport in mesoscopic devices

Tomi Ruokola

Doctoral dissertation for the degree of Doctor of Science in Technology to be presented with due permission of the School of Science for public examination and debate in Auditorium K at the Aalto University School of Science (Espoo, Finland) on the 17th of August 2012 at 13 o'clock.

Aalto University
School of Science
Department of Applied Physics

Supervising professor
Prof. Risto Nieminen

Thesis advisor
Dr. Teemu Ojanen

Preliminary examiners
Prof. Erkki Thuneberg, University of Oulu, Finland
Prof. Andreas Wacker, Lund University, Sweden

Opponent
Prof. Frank Hekking, Université Joseph Fourier, France

Aalto University publication series
DOCTORAL DISSERTATIONS 96/2012

ISBN 978-952-60-4714-0 (printed)
ISBN 978-952-60-4715-7 (pdf)
ISSN-L 1799-4934
ISSN 1799-4934 (printed)
ISSN 1799-4942 (pdf)
http://urn.fi/URN:ISBN:978-952-60-4715-7

Unigrafia Oy
Helsinki 2012

Finland

Author
Tomi Ruokola

Name of the doctoral dissertation
Thermal transport in mesoscopic devices

Publisher School of Science

Unit Department of Applied Physics

Series Aalto University publication series DOCTORAL DISSERTATIONS 96/2012

Field of research Condensed matter physics

Manuscript submitted 20 March 2012 **Date of the defence** 17 August 2012

Permission to publish granted (date) 4 May 2012 **Language** English

☐ **Monograph** ☒ **Article dissertation (summary + original articles)**

Abstract

New mechanisms for controlling heat flow and for converting heat to work in small-scale solid-state systems are highly desirable, particularly when considering the rapid miniaturization and ever-increasing power densities of electronic devices. Mesoscopic structures, being much larger than individual atoms but still small enough to exhibit some quantum-mechanical features, offer a versatile platform for studying thermal phenomena at reduced length scales.

We perform a theoretical study of two types of mesoscopic heat transport devices, namely heat rectifiers and heat engines. A rectifier is a device which allows heat to flow in one direction but flow in the other direction is suppressed. Two different rectifiers are proposed: one is a nonlinear oscillator controlling photonic heat flow in a microwave circuit, the other is a pair Coulomb blockade islands rectifying electronic heat currents. Particularly the latter device offers rectification performance unparallelled in the literature.

We also propose a new class of thermoelectric heat engines where electrons are transported between two reservoirs but heat is exchanged between the transport system and a third reservoir by microwave photons. Heat and charge flows are therefore separated, offering much greater flexibility than usual thermoelectrics. Also the two heat baths can be widely separated. With an appropriate setup this device can reach very high efficiencies.

Keywords heat transport, rectification, heat engine, microwave circuit, single-electron device

ISBN (printed) 978-952-60-4714-0 **ISBN (pdf)** 978-952-60-4715-7

ISSN-L 1799-4934 **ISSN (printed)** 1799-4934 **ISSN (pdf)** 1799-4942

Location of publisher Espoo **Location of printing** Helsinki **Year** 2012

Pages 92 **urn** http://urn.fi/URN:ISBN:978-952-60-4715-7

A! Aalto-yliopisto

Tiivistelmä

Aalto-yliopisto, PL 11000, 00076 Aalto www.aalto.fi

Tekijä
Tomi Ruokola

Väitöskirjan nimi
Lämmönkuljetusta mesoskooppisissa laitteissa

Julkaisija Perustieteiden korkeakoulu

Yksikkö Teknillisen fysiikan laitos

Sarja Aalto University publication series DOCTORAL DISSERTATIONS 96/2012

Tutkimusala Tiiviin aineen fysiikka

Käsikirjoituksen pvm 20.03.2012 **Väitöspäivä** 17.08.2012

Julkaisuluvan myöntämispäivä 04.05.2012 **Kieli** Englanti

☐ **Monografia** ☒ **Yhdistelmäväitöskirja (yhteenveto-osa + erillisartikkelit)**

Tiivistelmä

Uusien tapojen kehittäminen lämmönkuljetukseen ja lämmön muuntamiseen hyötyenergiaksi hyvin pienissä kiinteän olomuodon rakenteissa on olennainen teknologinen tavoite, etenkin kun huomioidaan elektronisten komponenttien nopea pienentymistrendi ja niiden alati kasvava lämmöntuottotiheys. Mesoskooppiset laitteet, jotka ovat kooltaan yksittäisiä atomeja huomattavasti suurempia mutta silti riittävän pieniä jotta kvanttimekaaniset ilmiöt on huomioitava, ovat monipuolinen alusta pienen mittakaavan lämpöilmiöiden tutkimiselle.

Tässä työssä tutkitaan teoreettisesti kahdenlaisia mesoskooppisia lämmönkuljetuslaitteita, lämpödiodeja ja lämpövoimakoneita. Lämpödiodi on laite joka sallii lämpöenergian virtauksen yhteen suuntaan mutta estää sen toiseen suuntaan. Väitös käsittelee kahta erilaista diodia: ensimmäisessä epälineaarinen oskillaattoripiiri kontrolloi fotonien kuljettamaa lämpöä, toisessa lämmön tasasuuntaukseen käytetään Coulombin saartoon perustuvia yksielektronisaarekkeita. Erityisesti jälkimmäinen laite on poikkeuksellisen suorituskykyinen.

Työssä käsitellään myös uudentyyppisiä lämpövoimakoneita, joiden toimintaperiaate poikkeaa olennaisesti perinteisistä lämpösähkögeneraattoreista. Ehdotetussa laitetyypissä elektronit tuottavat hyötytehon kulkemalla kahden samanlämpöisen metallin välillä, lämpö puolestaan tuodaan kolmannesta metallista mikroaaltofotonien välityksellä. Lämpö- ja sähkövirtojen erottaminen mahdollistaa monipuoliset rakenteelliset ratkaisut, esimerkiksi lämpölähteet voivat olla hyvinkin kaukana toisistaan. Saavutettavat hyötysuhteet ovat kuitenkin samoja kuin pelkästään elektroneihin perustuvissa laitteissa.

Avainsanat lämmönkuljetus, tasasuuntaus, lämpövoimakone, mikroaaltopiiri, yksielektronilaite

ISBN (painettu) 978-952-60-4714-0 **ISBN (pdf)** 978-952-60-4715-7

ISSN-L 1799-4934 **ISSN (painettu)** 1799-4934 **ISSN (pdf)** 1799-4942

Julkaisupaikka Espoo **Painopaikka** Helsinki **Vuosi** 2012

Sivumäärä 92 **urn** http://urn.fi/URN:ISBN:978-952-60-4715-7

Contents

List of Publications

This thesis consists of an overview and of the following publications which are referred to in the text by their Roman numerals.

I Tomi Ruokola and Teemu Ojanen. Thermal conductance in a spin-boson model: Cotunneling and low-temperature properties. *Physical Review B*, 83, 045417, January 2011.

II Tomi Ruokola, Teemu Ojanen, and Antti-Pekka Jauho. Thermal rectification in nonlinear quantum circuits. *Physical Review B*, 79, 144306, April 2009.

III Tomi Ruokola and Teemu Ojanen. Single-electron heat diode: Asymmetric heat transport between electronic reservoirs through Coulomb islands. *Physical Review B*, 83, 241404(R), June 2011.

IV Tomi Ruokola and Teemu Ojanen. Theory of single-electron heat engines coupled to electromagnetic environments. *Physical Review B*, submitted on 17 February 2012.

Author's Contribution

Publication I: "Thermal conductance in a spin-boson model: Cotunneling and low-temperature properties"

The author provided some of the ideas, performed the calculations and analysis, and wrote the paper with input from the coauthor.

Publication II: "Thermal rectification in nonlinear quantum circuits"

The author provided some of the ideas, performed the calculations and analysis, and wrote the paper with input from the coauthors.

Publication III: "Single-electron heat diode: Asymmetric heat transport between electronic reservoirs through Coulomb islands"

The author provided some of the central ideas, performed the calculations and analysis, and wrote the paper with input from the coauthor.

Publication IV: "Theory of single-electron heat engines coupled to electromagnetic environments"

The author provided all of the ideas, performed the calculations and analysis, and wrote the paper with input from the coauthor.

1. Introduction

1.1 Thermal mesoscopics

Understanding how heat is transported and converted to other forms of energy is an important scientific problem that is being studied in many fields from theoretical physics to civil engineering. Mesoscopic structures, being larger than atomic systems but still exhibiting some quantum phenomena, are in many ways ideal testbeds for investigating thermal physics [1]. Firstly, new mechanisms for controlling heat flow emerge when matter can be manipulated at the microscale, and unlike individual atoms or molecules, mesoscopic systems can be readily engineered to given specifications. Secondly, the miniaturization trend in technology will result in an ever increasing number of different microscopic devices, and it is therefore imperative to have a thorough understanding of thermal management at these reduced length scales. Finally, the effective state space of mesoscopic devices can be made small enough to facilitate the investigation of fundamental limits of heat transport phenomena.

In solid-state systems heat can be transported by several types of excitations. Lattice vibrations, or phonons, are very important carriers of heat since they are always present in solid materials. However, devices with some useful functionality essentially always require the possibility to control the system with external fields, and also a nonlinear response is often needed. But these properties can be difficult to achieve with phonons since they generally interact rather weakly with other phonons or with electromagnetic fields, and for this reason we do not consider phononic systems in this thesis. On the other hand, in electrically conducting materials mobile electrons provide an important contribution to thermal conductivity. From the point of view of mesoscopics, charge transport by electrons is a

well-established field and one can readily adapt these methods and ideas also to heat transport. As an example of this, in Section 3.3 we introduce a setup where heat flow between two reservoirs is controlled by Coulomb blockade physics. Finally, heat can also be exchanged by thermal radiation. This is usually not a relevant conduction channel in solid-state systems but in some cases it is possible for both electronic and phononic heat flows to become suppressed and then the photonic channel will dominate [2]. At low temperatures, around a few Kelvins or below, thermal radiation is carried by microwave photons which can be controlled in a very versatile manner by techniques familiar from microwave engineering.

1.2 Heat currents in low-dimensional systems

An outstanding feature of transport in mesoscopic physics is conductance quantization: when propagating through systems with restricted dimensions, particles can only have discrete values for their transverse momentum, with each transverse mode corresponding to one conductance channel. It can then be shown that one channel can only carry a certain maximum current. For the transport of electrical charge this quantization is well known and has been demonstrated already more than 20 years ago [3, 4]. Similar quantization applies also for heat transport. The maximum heat current for a single channel can most conveniently be derived by considering the Landauer formula [5, 6] for elastic transport between two electron reservoirs, L and R, but with the electric charge replaced with the electron energy:

$$J = \int_{-\infty}^{\infty} \frac{d\varepsilon}{2\pi\hbar} \varepsilon \mathcal{T}(\varepsilon)[f_L(\varepsilon) - f_R(\varepsilon)] \tag{1.1}$$

where $f_\alpha(\varepsilon) \equiv (e^{\varepsilon/k_B T_\alpha} + 1)^{-1}$ is the Fermi function for reservoir $\alpha = L,\ R$, and $\mathcal{T}$ is the transmission function. Note that the system is unbiased so that no Joule heating is involved. We can also consider the corresponding formula for bosons [7]:

$$J = \int_{0}^{\infty} \frac{d\omega}{2\pi} \hbar\omega \mathcal{T}(\omega)[n_L(\omega) - n_R(\omega)] \tag{1.2}$$

where $n_\alpha(\omega) \equiv (e^{\hbar\omega/k_B T_\alpha} - 1)^{-1}$ are the reservoir Bose functions. Notice the different integration limits in the above two equations. If we now assume full transmission by setting $\mathcal{T} = 1$, in both cases integration gives [7, 8]

$$J_Q = \frac{\pi k_B^2}{12\hbar}(T_L^2 - T_R^2) \tag{1.3}$$

as the maximum heat current for one quantized channel. This result has actually been shown to apply for heat carried by excitations of any statistics [9], and it has also been experimentally demonstrated for electrons [10], phonons [11], and photons [12, 13]. All the systems considered in this thesis are single-channel conductors and therefore Eq. (1.3) gives an upper limit for the achievable heat currents.

1.3 Outline

Chapter 2 forms the theoretical foundation of this Thesis. There we introduce the transport methods that are used to study the devices introduced in the later Chapters. We consider two methods that are appropriate for interacting systems, namely nonequilibrium Green's functions and master equations with Fermi golden rule. We go through a simple pedagogical example of transport through a harmonic oscillator, which allows a convenient comparison between the different approaches. We also consider heat flow through a two-level system with a higher-order generalization of the golden rule.

In Chapter 3 we investigate devices which are able to rectify heat currents. After introducing some metrics for evaluating the diode performance, we consider two new device designs: a photonic rectifier transporting heat with microwave radiation and a single-electron diode using Coulomb blockade for heat transport. The latter system is shown to have a particularly impressive rectification performance.

Chapter 4 discusses heat engines of the thermoelectric type. After reviewing the properties of a basic two-reservoir device, we introduce a three-reservoir heat engine where work is performed by electrons but heat is carried by photons. Similarities and differences between these two device types are examined.

In Chapter 5 we summarize our results and point out important open problems.

For the rest of the Thesis we use natural units with $k_B = \hbar = e = 1$.

2. Methods for heat transport

Transport in mesoscopic systems can be studied by a variety formalisms. In the Introduction we already encountered the Landauer-type scattering approach which, however, is directly applicable only for noninteracting transport [6]. Interactions are essential for the devices we wish to study and therefore we consider two widely-used methods capable of handling interacting systems, namely nonequilibrium Green's functions and master equations with Fermi golden rule transition rates. In both of these methods the system is conceptually divided into left (L) and right (R) reservoirs which are taken to be noninteracting and in thermal equilibrium, and a central device (C) which can be interacting and out of equilibrium. We will see that the Green's function approach is best suited for the case when the different system parts are strongly coupled while the master equation method is suitable for weak coupling.

Both methods can equally well treat electronic and photonic transport but in this chapter we introduce them by considering a simple photonic system, depicted in Fig. 2.1. It is assumed that the wavelength of thermal photons is much larger than the circuit dimensions so that we can treat the different parts of the system as lumped elements. For example, at 1 Kelvin the circuit must be smaller than 1 centimeter, which is easily achieved. Then the linear reservoirs can be described with admittances $Y_{L/R}(\omega)$, while the central device is an LC oscillator with frequency $\omega_0 = 1/\sqrt{LC}$. The reservoir circuits are coupled to the central oscillator via mutual inductances $M_{L/R}$, allowing electromagnetic fluctuations to transmit heat between the thermal baths, held at temperatures $T_{L/R}$. This fully linear circuit has the advantageous feature that heat transport through the system can be solved exactly by using just classical circuit theory supplemented with fluctuation–dissipation theorem. We perform this calculation in Section 2.1, and the results are then used to bench-

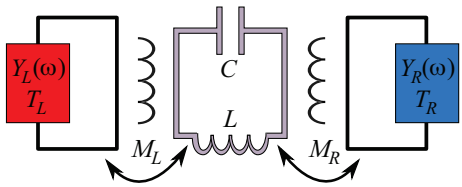

Figure 2.1. Example system used for presenting the different transport methods. It consists of linear reservoirs with arbitrary admittances $Y_{L,R}(\omega)$, and a harmonic LC oscillator as a central device. The reservoirs are coupled to the oscillator through mutual inductances $M_{L,R}$. Electromagnetic fluctuations transmit heat through the system between the reservoirs which have different temperatures $T_{L,R}$.

mark the other two methods, nonequilibrium Green's functions in Section 2.2 and master equations with golden rule in Section 2.3. Finally in Section 2.4 we consider another setup with a two-level system as the central device and show how a generalization of the golden rule can be used to treat higher-order tunneling effects.

2.1 Classical circuit theory

According to the fluctuation–dissipation theorem [14], a dissipative system, like the reservoir α with admittance Y_α in Fig. 2.1, always exhibits spontaneous fluctuations. For present purposes it is useful to separate these two aspects into two different circuit elements, namely a purely passive admittance Y_α in parallel with a fluctuating current source δI_α. The average current vanishes, $\langle \delta I_\alpha \rangle = 0$, while the noise is given by the Johnson–Nyquist expression [14]:

$$\langle \delta I_\alpha(\omega) \delta I_\alpha^*(\omega) \rangle = 4\omega \mathbf{Re}[Y_\alpha(\omega)][n_\alpha(\omega) + \frac{1}{2}] \tag{2.1}$$

which uses the (classical) convention that ω is limited to positive values and both emission and absorption noise are included for given ω. A current fluctuation δI_L in the left reservoir propagates through the circuit and in turn induces a voltage fluctuation ΔV_R between the terminals of Y_R. Since the system is linear and time-independent, these two fluctuations are related simply by $\Delta V_R(\omega) = Z(\omega)\delta I_L(\omega)$, and a circuit theory calculation shows that

$$Z(\omega) = \frac{M_L M_R \omega^2}{Z_c(\omega) + M_L^2 \omega^2 Y_L(\omega) + M_R^2 \omega^2 Y_R(\omega)} \tag{2.2}$$

where the series impedance of the central oscillator is $Z_c(\omega) = -iL(\omega^2 - \omega_0^2)/\omega$. The corresponding current fluctuation through the right reservoir

is $\Delta I_R(\omega) = Y_R(\omega)\Delta V_R(\omega)$, and the absorbed average power at frequency ω is

$$\begin{aligned} j_{L\to R}(\omega) &= \mathrm{Re}\,\langle \Delta V_R(\omega)\Delta I_R^*(\omega)\rangle \\ &= |Z(\omega)|^2 \mathrm{Re}[Y_R(\omega)]\langle \delta I_L(\omega)\delta I_L^*(\omega)\rangle \end{aligned} \tag{2.3}$$

which can be interpreted as the spectral density of heat current flowing from left to right. Because fluctuations in the two reservoirs are independent, current in the other direction is obtained simply by swapping L and R in Eq. (2.3). Collecting everything gives the total heat current as [15]

$$\begin{aligned} J &= \int_0^\infty \frac{d\omega}{2\pi}[j_{L\to R}(\omega) - j_{R\to L}(\omega)] \\ &= \int_0^\infty \frac{d\omega}{2\pi} \frac{4\omega\Gamma_L(\omega)\Gamma_R(\omega)[n_L(\omega) - n_R(\omega)]}{\left|\frac{\omega^2-\omega_0^2}{\omega_0} + i\Gamma(\omega) - \Lambda(\omega)\right|^2} \end{aligned} \tag{2.4}$$

where we have introduced the functions

$$\Gamma_\alpha(\omega) = M_\alpha^2 C\omega_0\omega^3 \mathrm{Re}[Y_\alpha(\omega)] \tag{2.5}$$

$$\Lambda_\alpha(\omega) = M_\alpha^2 C\omega_0\omega^3 \mathrm{Im}[Y_\alpha(\omega)] \tag{2.6}$$

and $\Gamma = \Gamma_L + \Gamma_R$, $\Lambda = \Lambda_L + \Lambda_R$. Reason for this notation becomes clear in the following sections when we compare the results from quantum transport calculations to Eq. (2.4).

We also note that Eq. (2.4) can be written in the form of Eq. (1.2) with $\mathcal{T}(\omega) \le 4\Gamma_L(\omega)\Gamma_R(\omega)/[\Gamma_L(\omega)+\Gamma_R(\omega)]^2$, where the upper bound is attained in the limit $\Gamma(\omega) \gg (\omega^2 - \omega_0^2)/\omega_0 - \Lambda(\omega)$. Then if the system is symmetric, $\Gamma_L = \Gamma_R$, we have $\mathcal{T}(\omega) \to 1$. Therefore the value of Eq. (2.4) is limited by the heat current quantum J_Q of Eq. (1.3).

2.2 Nonequilibrium Green's functions

For a quantum-mechanical treatment we need to write down the Hamiltonian corresponding to the system in Fig. 2.1. The central circuit is a simple harmonic oscillator and the linear baths can also be described as collections of oscillators with a linear coupling to the central part:

$$H = H_C + H_L + H_R + H_T \tag{2.7}$$

$$H_C = \frac{1}{2}\omega_0(X^2 + P^2) \tag{2.8}$$

$$H_\alpha = \sum_{j\in\alpha} \frac{1}{2}\omega_j(x_j^2 + p_j^2), \quad \alpha = L, R \tag{2.9}$$

$$H_T = \sum_{j\in L,R} c_j x_j X \tag{2.10}$$

where (X, P) and (x_j, p_j) are the dimensionless canonical positions and momenta of the central oscillator and the reservoir oscillators, obeying $[X, P] = [x_j, p_j] = i$. In terms of the ladder operators they are given as $x_j = (a_j + a_j^\dagger)/\sqrt{2}$ and $p_j = -i(a_j - a_j^\dagger)/\sqrt{2}$. Connection between the parameters in Eqs. (2.8)–(2.10) and the physical quantities in Fig. 2.1 is made further below.

We now show how to calculate the heat current through the system with nonequilibrium Green's functions. This formalism is covered in detail in the textbook by Haug and Jauho [16] and our derivation here will roughly follow the book, with electrons replaced by harmonic oscillators. The Green's function method for circuit photons was first considered in Ref. [17], and it has also been used for *phononic* heat transport [18].

Let us introduce the formalism by considering the *equilibrium* Green's functions for the reservoir oscillators. Equilibrium is achieved by setting $c_i = 0$, and we indicate this with a subscript 0 in the relevant quantities. First, the greater two-point Green's function for x_j is defined as

$$\langle x_j, x_j\rangle_0^>(t - t') \equiv -i\langle x_j(t)x_j(t')\rangle_0 \tag{2.11}$$

In other words, it is the expectation value of the product of the x_j operators at two different times, and due to time-translation invariance it only depends on the time difference $t - t'$. For time evolution the Heisenberg picture in employed. Now using the fact that for an uncoupled reservoir the time dependence of the lowering operator is $a_j(t) = a_j e^{-i\omega_j t}$, and the fact that in thermal equilibrium the density matrix is diagonal with $\langle a_j^\dagger a_j\rangle_0 = n(\omega_j)$, the Fourier transformed Green's function is

$$\langle x_j, x_j\rangle_0^>(\omega) = -i\pi[n(\omega) + 1][\delta(\omega - \omega_j) - \delta(\omega + \omega_j)] \tag{2.12}$$

The lesser Green's function is obtained by swapping the two operators:

$$\langle x_j, x_j\rangle_0^<(t - t') \equiv -i\langle x_j(t')x_j(t)\rangle_0 \tag{2.13}$$

Now a Fourier transform yields

$$\langle x_j, x_j\rangle_0^<(\omega) = -i\pi n(\omega)[\delta(\omega - \omega_j) - \delta(\omega + \omega_j)] \tag{2.14}$$

The retarded Green's function is defined as the retarded part $(t > t')$ of the commutator of $x_j(t)$ and $x_j(t')$:

$$\langle x_j, x_j\rangle_0^r(t - t') \equiv -i\theta(t - t')\langle[x_j(t), x_j(t')]\rangle_0 \tag{2.15}$$

$$\langle x_j, x_j\rangle_0^r(\omega) = -\frac{i\pi}{2}[\delta(\omega - \omega_j) - \delta(\omega + \omega_j)] + \mathcal{P}\frac{\omega_j}{\omega^2 - \omega_j^2} \tag{2.16}$$

where $\mathcal{P}$ denotes the Cauchy principal value. The advanced Green's function is defined in a similar way but taking the advanced part:

$$\langle x_j, x_j\rangle_0^a(t-t') \equiv i\theta(t'-t)\langle[x_j(t), x_j(t')]\rangle_0 \tag{2.17}$$

$$\langle x_j, x_j\rangle_0^a(\omega) = \frac{i\pi}{2}[\delta(\omega-\omega_j)-\delta(\omega+\omega_j)] + \mathcal{P}\frac{\omega_j}{\omega^2-\omega_j^2} \tag{2.18}$$

Finally the time-ordered Green's function is

$$\langle x_j, x_j\rangle_0^t(t-t') \equiv -i\langle T\{x_j(t)x_j(t')\}\rangle_0 \tag{2.19}$$

$$= \theta(t-t')\langle x_j, x_j\rangle_0^>(t-t') + \theta(t'-t)\langle x_j, x_j\rangle_0^<(t-t')$$

$$\langle x_j, x_j\rangle_0^t(\omega) = \frac{\omega_j}{\omega^2-\omega_j^2} \tag{2.20}$$

where T is the time-ordering operator. We must emphasize that the time-domain definitions are generic, that is, they apply also in nonequilibrium, while the Fourier transforms given above are only applicable in equilibrium. By inspecting the definitions, one can come up with several relationships connecting the different Green's functions. These will be introduced below when needed.

Now we are prepared to evaluate the heat current within the *nonequilibrium* Green's function framework, so the couplings in H_T are restored. We start by noting that the heat flow from left to right is the negative energy change of the left reservoir, that is,

$$J = -\langle \dot{H}_L\rangle = -\sum_{j\in L}\omega_j\langle x_j\dot{x}_j + p_j\dot{p}_j\rangle = \sum_{j\in L} c_j\langle \dot{x}_j X\rangle \tag{2.21}$$

where we have used the time derivatives $\dot{x}_j \equiv -i[x_j, H] = \omega_j p_j$ and $\dot{p}_j = -\omega_j x_j - c_j X$. The last expectation value in Eq. (2.21) can be expressed in terms of a mixed lesser Green's function of x_j and X:

$$\langle \dot{x}_j(t)X(t)\rangle = i\lim_{t'\to t}\partial_t\langle x_j, X\rangle^<(t-t') = \int_{-\infty}^{\infty}\frac{d\omega}{2\pi}\omega\langle x_j, X\rangle^<(\omega) \tag{2.22}$$

so that

$$J = \int_{-\infty}^{\infty}\frac{d\omega}{2\pi}\omega\sum_{j\in L} c_j\langle x_j, X\rangle^<(\omega) \tag{2.23}$$

By differentiating the corresponding time-ordered Green's function we get

$$(i\partial_t)^2\langle x_j, X\rangle^t(t-t') = \omega_j^2\langle x_j, X\rangle^t(t-t') + \omega_j c_j\langle X, X\rangle^t(t-t') \tag{2.24}$$

and then a Fourier transform gives

$$\langle x_j, X\rangle^t(\omega) = c_j\langle x_j, x_j\rangle_0^t(\omega)\langle X, X\rangle^t(\omega) \tag{2.25}$$

where we have used Eq. (2.20). With analytic continuation methods on the Keldysh contour one can obtain so-called Langreth rules giving relationships between different nonequilibrium Green's functions [16]. One

of these rules states that if three Green's functions are related in the frequency domain as $A^t = B^t C^t$, then we have $A^< = B^r C^< + B^< C^a$. Applying this to Eq. (2.25), we can write Eq. (2.23) as

$$J = \int_{-\infty}^{\infty} \frac{d\omega}{2\pi} \omega \left[G^<(\omega)\Sigma_L^r(\omega) + G^a(\omega)\Sigma_L^<(\omega) \right] \tag{2.26}$$

where we have defined the center oscillator Green's function as $G \equiv \langle X, X \rangle$ and the self-energy for coupling to reservoir α as $\Sigma_\alpha \equiv \sum_{j\in\alpha} c_j^2 \langle x_j, x_j \rangle_0$. Since heat current is a real quantity, the bracketed expression in Eq. (2.26) must be equal to its real part. From the definitions of the different Green's functions one can see that $[G^{r/a}(\omega)]^* = G^{a/r}(\omega)$, $[G^{</>}(\omega)]^* = -G^{</>}(\omega)$, and $G^r - G^a = G^> - G^<$. Then we have

$$\begin{aligned} \mathrm{Re}[G^<\Sigma_L^r + G^a\Sigma_L^<] &= \frac{1}{2}[G^<\Sigma_L^r - G^<\Sigma_L^a + G^a\Sigma_L^< - G^r\Sigma_L^<] \\ &= \frac{1}{2}[G^<\Sigma_L^> - G^>\Sigma_L^<] \end{aligned}$$

Furthermore the definitions show that for a time-translation invariant system $G^>(\omega) = G^<(-\omega)$, and therefore the integrand $\omega[G^<(\omega)\Sigma_L^>(\omega) - G^>(\omega)\Sigma_L^<(\omega)]$ is even. Combining these observations results in

$$J = \int_0^{\infty} \frac{d\omega}{2\pi} \omega \left[G^<(\omega)\Sigma_L^>(\omega) - G^>(\omega)\Sigma_L^<(\omega) \right] \tag{2.27}$$

This equation applies for an arbitrary central device since we have not used any properties of H_C while deriving it. Next we note that from the time-evolution equation for G one can obtain the Keldysh formula [16]

$$G^{</>} = G^r \Sigma^{</>} G^a \tag{2.28}$$

where $\Sigma = \Sigma_L + \Sigma_R + \Sigma_{int}$ is the total self-energy of the central part. When the system is non-interacting (or interactions are treated in a mean-field approximation, which is formally the same thing), the interaction self-energy vanishes, $\Sigma_{int} = 0$. The bracketed term in Eq. (2.27) then becomes $G^<\Sigma_L^> - G^>\Sigma_L^< = |G^r|^2(\Sigma_L^>\Sigma_R^< - \Sigma_L^<\Sigma_R^>)$. The different forms of the self-energies can be obtained from Eqs. (2.12), (2.14), and (2.16):

$$\Sigma_\alpha^<(\omega) = -2i\Gamma_\alpha(\omega) n_\alpha(\omega) \tag{2.29}$$

$$\Sigma_\alpha^>(\omega) = -2i\Gamma_\alpha(\omega)[n_\alpha(\omega) + 1] \tag{2.30}$$

$$\Sigma_\alpha^r(\omega) = -i\Gamma_\alpha(\omega) + \Lambda_\alpha(\omega) \tag{2.31}$$

with

$$\Gamma_\alpha(\omega) = \frac{\pi}{2} \sum_{j\in\alpha} c_j^2 [\delta(\omega - \omega_j) - \delta(\omega + \omega_j)] \tag{2.32}$$

$$\Lambda_\alpha(\omega) = \sum_{j\in\alpha} c_j^2 \mathcal{P} \frac{\omega_j}{\omega^2 - \omega_j^2} \tag{2.33}$$

We then have

$$J = \int_0^\infty \frac{d\omega}{2\pi} 4\omega |G^r(\omega)|^2 \Gamma_L(\omega)\Gamma_R(\omega)[n_L(\omega) - n_R(\omega)] \tag{2.34}$$

We must still calculate the expression for G^r. An equation-of-motion analysis, similar to Eq. (2.24), reveals that

$$(i\partial_t)^2 G^r(t-t') = \omega_0^2 G^r(t-t') + \omega_0 \sum_{j\in L,R} c_j \langle x_j, X\rangle^r(t-t') + \omega_0 \delta(t-t') \tag{2.35}$$

We note that Eq. (2.25) applies also for retarded Green's functions. Then substituting that in Eq. (2.35) and Fourier transforming, we have the Green's function for a coupled harmonic oscillator:

$$G^r(\omega) = \left(\frac{\omega^2 - \omega_0^2}{\omega_0} - \Sigma_L^r(\omega) - \Sigma_R^r(\omega) \right)^{-1} \tag{2.36}$$

The final expression for the heat current can now be obtained [17]:

$$J = \int_0^\infty \frac{d\omega}{2\pi} \frac{4\omega\Gamma_L(\omega)\Gamma_R(\omega)[n_L(\omega) - n_R(\omega)]}{\left| \frac{\omega^2-\omega_0^2}{\omega_0} + i\Gamma(\omega) - \Lambda(\omega) \right|^2} \tag{2.37}$$

where $\Gamma = \Gamma_L + \Gamma_R$ and $\Lambda = \Lambda_L + \Lambda_R$. This result is an exact consequence of the Hamiltonian (2.7), no approximations have been made. Before it can be compared to Eq. (2.4) we must find the connection between the Γ and Λ functions given by Eqs. (2.5)–(2.6) and Eqs. (2.32)–(2.33). We proceed by writing the Hamiltonian (2.7) in terms of the physical circuit parameters. Since the central device is an LC resonator with $\omega_0 = 1/\sqrt{LC}$, its Hamiltonian can be written as

$$H_C = \frac{Q^2}{2C} + \frac{\phi^2}{2L} \tag{2.38}$$

where Q is the charge on the capacitor and ϕ the flux in the inductor. In order to match this to Eq. (2.8) we should write Q and ϕ in terms of X and P. If the Hamiltonian consisted only of the central oscillator, Q could be chosen to be any linear combination of X and P. However, in this case we also have a coupling to the reservoir circuits given by Eq. (2.10), and as shown below, the Kirchhoff rules are given correctly only if Q is proportional to X. Then comparing Eq. (2.38) to Eq. (2.8) gives

$$\begin{aligned} Q &= \sqrt{C\omega_0} X \\ \phi &= \sqrt{L\omega_0} P \end{aligned} \tag{2.39}$$

Now the equations of motion for Q and ϕ are obtained from Eqs. (2.7)–(2.10) and (2.39):

$$\dot{Q} = \frac{\phi}{L} \tag{2.40}$$

$$\dot{\phi} = -\frac{Q}{C} - \sqrt{L\omega_0} \sum_{j\in L,R} c_j x_j \tag{2.41}$$

The first equation gives the current conservation in the circuit loop. If Q had a nonvanishing P component this would be violated and thus Q must be proportional to X. The second equation is the Kirchhoff voltage law, with the last term giving the voltages produced by the inductive coupling to the reservoir circuits. On the other hand, the flux ϕ_α induced in the resonator by current I_α in reservoir α is $\phi_\alpha = M_\alpha I_\alpha$, and we can write

$$\dot{\phi}_\alpha = \sqrt{L\omega_0} \sum_{j\in\alpha} c_j x_j = \partial_t (M_\alpha I_\alpha) \tag{2.42}$$

This equation fixes the relationship between the formal coupling constants c_j and the physical parameters $M_{L,R}$, L, and C.

Finally, the reservoir admittances are related to the retarded current–current correlators via the Kubo formula [19]:

$$\begin{aligned} Y_\alpha(\omega) &= \frac{i\langle I_\alpha, I_\alpha\rangle_0^r(\omega)}{\omega} \\ &= \frac{L\omega_0}{M_\alpha^2\omega^3} \sum_{j\in\alpha} c_j^2 i\langle x_j, x_j\rangle_0^r(\omega) \\ &= \frac{\Gamma_\alpha(\omega) + i\Lambda_\alpha(\omega)}{M_\alpha^2 C\omega_0\omega^3} \end{aligned} \tag{2.43}$$

In the second equality we have used the Fourier transform of Eq. (2.42), and in the last equality we have used Eqs. (2.16), (2.32), and (2.33). From this we see that Γ_α and Λ_α from Eqs. (2.32) and (2.33), written in terms of the circuit parameters, match exactly those given in Eqs. (2.5) and (2.6), and therefore Eqs. (2.4) and (2.37) can be directly compared. Since these equations are identical, we can conclude that the Green's function method has produced an exact result which is to be expected since no approximations have been made.

The nonequilibrium Green's function method is used in Section 3.2 and in Publication **II** to study thermal rectification through a weakly nonlinear oscillator.

2.3 Master equations with Fermi golden rule

A particularly simple description for the system dynamics can be obtained in the weak-coupling limit when the density matrix of the central oscillator can be taken to be diagonal at all times. Then the state of the system is uniquely determined by the probabilities P_N to have an N-boson excitation of the oscillator, and their time evolution is given by the master equation

$$\dot{P}_N = -(\Gamma_{\downarrow,N} + \Gamma_{\uparrow,N})P_N + \Gamma_{\uparrow,N-1}P_{N-1} + \Gamma_{\downarrow,N+1}P_{N+1} \tag{2.44}$$

where $\Gamma_{\uparrow(\downarrow),N}$ is the rate that the reservoirs excite (de-excite) the oscillator with occupation N. Once the rates are known, the steady-state solution ($\dot{P}_N = 0$) for P_N follows immediately. Then the heat current from left to right can then be calculated as the rate of energy emitted minus the rate of energy absorbed by the left reservoir. If we operate in a regime where higher-order tunneling processes, carrying heat between the reservoirs without exciting the central oscillator, can be neglected, heat current can be written as

$$J = \omega_0 \sum_{N=0}^{\infty} \Gamma_{L\uparrow,N} P_N - \omega_0 \sum_{N=1}^{\infty} \Gamma_{L\downarrow,N} P_N \tag{2.45}$$

where we have split the excitation rates between the two reservoirs as $\Gamma_{\updownarrow,N} = \Gamma_{L\updownarrow,N} + \Gamma_{R\updownarrow,N}$ and used the fact that each oscillator excitation carries energy ω_0.

The lowest-order tunneling rates required by Eqs. (2.44) and (2.45) are most simply calculated with the help of the Fermi golden rule [19]

$$\Gamma_{i\to f} = 2\pi |\langle f|H_T|i\rangle|^2 \delta(E_i - E_f) \tag{2.46}$$

where H_T is the tunneling element connecting the initial and final states $|i\rangle$ and $|f\rangle$, having energies E_i and E_f. Let us now see how this can be applied to the oscillator system, Eq. (2.7), that we have been studying. We start by considering the case where the central oscillator, with an initial occupation of N, absorbs one boson from reservoir α. Initially the reservoir is in thermal equilibrium, being in state $|R_i\rangle$ with probability W_i, while the central device is in state $|N\rangle$. Then one boson from reservoir oscillator j is absorbed, exciting the central system. The resulting normalized final state is

$$|f\rangle = \frac{a_j b^\dagger}{\sqrt{N_{j,i}(N+1)}} |R_i\rangle|N\rangle \tag{2.47}$$

where b and a_j are annihilation operators for the central and reservoir modes, and $N_{j,i}$ is the occupation of oscillator j in state $|R_i\rangle$. The rate for the absorption process is now given by Eq. (2.46), summed over all possible reservoir states and oscillators:

$$\begin{aligned}
\Gamma_{\alpha\uparrow,N} &= 2\pi \sum_{i,j\in\alpha} \frac{|\langle N|\langle R_i|ba_j^\dagger H_T|R_i\rangle|N\rangle|^2}{N_{j,i}(N+1)} W_i \delta(\omega_0 - \omega_j) \\
&= \frac{|\langle N|bb^\dagger|N\rangle|^2}{N+1} \sum_{i,j\in\alpha} \frac{\langle R_i|a_j^\dagger a_j|R_i\rangle|^2}{N_{j,i}} W_i \frac{\pi}{2} c_j^2 \delta(\omega_0 - \omega_j) \\
&= \Gamma_\alpha(\omega_0) n_\alpha(\omega_0)(N+1)
\end{aligned} \tag{2.48}$$

where in the last line we have used the fact that $\sum_i N_{j,i} W_i = n_\alpha(\omega_j)$ and substituted Γ_α from Eq. (2.32). Similar calculation shows that the rate for

emitting one quantum from an N-occupied oscillator into reservoir α is

$$\Gamma_{\alpha\downarrow,N} = \Gamma_\alpha(\omega_0)[n_\alpha(\omega_0)+1]N \tag{2.49}$$

In the following it is useful to split off the N-dependence, and we define $\Gamma_{\alpha\uparrow} = \Gamma_\alpha(\omega_0)n_\alpha(\omega_0)$, $\Gamma_{\alpha\downarrow} = \Gamma_\alpha(\omega_0)[n_\alpha(\omega_0)+1]$, and $\Gamma_\updownarrow = \Gamma_{L\updownarrow} + \Gamma_{R\updownarrow}$. Equation (2.44) in steady state is now

$$0 = -(N\Gamma_\downarrow + (N+1)\Gamma_\uparrow)P_N + N\Gamma_\uparrow P_{N-1} + (N+1)\Gamma_\downarrow P_{N+1} \tag{2.50}$$

Following Ref. [20], solution of this system can be attempted with the ansatz $P_N = ay^N$ which leads to $y = \Gamma_\uparrow/\Gamma_\downarrow$ with the normalization $a = 1/(\sum_{N=0}^\infty y^N) = (1-y)$. Heat current can then be calculated from Eq. (2.45):

$$\begin{aligned} J &= \omega_0 \sum_{N=0}^\infty \Gamma_{L\uparrow}(N+1)P_N - \omega_0 \sum_{N=1}^\infty \Gamma_{L\downarrow} N P_N \\ &= \omega_0(\Gamma_{L\uparrow} - \Gamma_{L\downarrow} y)(1-y)\sum_{N=1}^\infty N y^{N-1} \\ &= \omega_0 \frac{\Gamma_\downarrow\Gamma_{L\uparrow} - \Gamma_\uparrow\Gamma_{L\downarrow}}{\Gamma_\downarrow - \Gamma_\uparrow} \end{aligned}$$

where we have used $\sum_{N=0}^\infty N y^{N-1} = (1-y)^{-2}$. Final simplification with Eqs. (2.48) and (2.49) then yields [20]

$$J = \omega_0 \frac{\Gamma_L(\omega_0)\Gamma_R(\omega_0)}{\Gamma_L(\omega_0)+\Gamma_R(\omega_0)}[n_L(\omega_0) - n_R(\omega_0)] \tag{2.51}$$

as the lowest-order, sequential tunneling heat current through a harmonic oscillator. The same result is also obtained from the exact result of Eq. (2.4) if transport only takes place at energy ω_0. This can be confirmed by writing Eq. (2.4) in the form

$$J = \int_0^\infty \frac{d\omega}{2\pi} \frac{4\omega\Gamma_L(\omega)\Gamma_R(\omega)[n_L(\omega) - n_R(\omega)]}{\left|\frac{(\omega+\omega_0)\omega_0}{\omega^2}\right|^2 \left|\omega - \omega_0 + \frac{\omega^2}{(\omega+\omega_0)\omega_0}\big(i\Gamma(\omega) - \Lambda(\omega)\big)\right|^2} \tag{2.52}$$

If we now assume that the couplings are weak, $\Gamma, \Lambda \ll \omega_0$, then the fact that

$$|\omega - \omega_0 - i\tilde{\Gamma}|^{-2} \to \frac{\pi}{\tilde{\Gamma}}\delta(\omega - \omega_0) \quad \text{when} \quad \tilde{\Gamma} \to 0 \tag{2.53}$$

can be used to reduce Eq. (2.52) to Eq. (2.51). Thus for weakly coupled systems it is reasonable to use the technically simple golden-rule approach but systems with stronger couplings require the nonequilibrium Green's function method.

The golden-rule master equation approach is employed in the next section and in Publication **I** for heat transport through a two-level system. Master equation for an electron system is used in Sections 3.3 and 4.2, and in Publications **III** and **IV** for studying single-electron thermal devices.

2.4 Generalized Fermi golden rule

The framework of master equations with golden rules rates can be extended to higher-order tunneling effects. The key ingredient here is the generalized version of the Fermi golden rule [19]:

$$\Gamma_{i\to f} = 2\pi|\langle f|T(E_i)|i\rangle|^2\delta(E_i - E_f) \tag{2.54}$$

where the scattering operator is

$$T(E) = H_T + H_T G_0(E) H_T + H_T G_0(E) H_T G_0(E) H_T + \ldots \tag{2.55}$$

Here G_0 is the retarded propagator for the uncoupled Hamiltonian $H_0 = H - H_T$:

$$G_0(E) = \frac{1}{E - H_0 + i\eta} \tag{2.56}$$

where η is a positive infinitesimal.

In contrast to the harmonic oscillator of the previous sections, we now wish to examine a two-level system (TLS) as the central device. A TLS coupled to a bosonic bath, known as the spin–boson model, is one of the most thoroughly studied model systems in physics due to its simplicity and generality: a TLS is the smallest (in terms of Hilbert space size) nontrivial quantum system, and in many cases nonlinear systems can be truncated to the two lowest states, giving a TLS. However, a *nonequilibrium* spin–boson model, where the spin is coupled to *two* different bosonic baths, has received much less attention [20, 21, 22, 23, 24, 25, 26, 27, 28]. Here and in Publication **I** we study heat transport through a TLS by using the generalized golden rule of Eq. (2.54).

The spin–boson Hamiltonian with two baths, L and R, is $H = H_0 + H_T$, where

$$H_0 = \tfrac{1}{2}\omega_0\sigma_z + \sum_{j\in L,R} \omega_j(a_j^\dagger a_j + \tfrac{1}{2}), \tag{2.57}$$

$$H_T = \sigma_x \sum_{j\in L,R} c_j(a_j + a_j^\dagger) \tag{2.58}$$

Next we must decide what kind tunneling processes we wish to study. For example, to calculate the transmission rate for a process where one boson is absorbed from the left and one emitted to the right, the initial and final states are related as

$$|f\rangle = \frac{1}{\sqrt{(N_{j_R,i}+1)N_{j_L,i}}}\, a_{j_R}^\dagger a_{j_L}|i\rangle, \tag{2.59}$$

where j_L and j_R are oscillators in the left and right bath, while $N_{j_L,i}$ and $N_{j_R,i}$ are their occupations in state $|i\rangle$. Equation (2.58) shows that each

tunneling event flips the spin and therefore $|i\rangle$ and $|f\rangle$ must have the same spin for a two-boson process. Note that here we consider energy transmission through the whole device whereas in Eq. (2.47) we only consider the tunneling between a reservoir and the resonator. If we would like to calculate the rate for the absorption and emission of two bosons between the baths, we would have $|f\rangle \sim a^\dagger_{j_R1} a^\dagger_{j_R2} a_{j_L1} a_{j_L2} |i\rangle$, etc. Here we continue with Eq. (2.59). It restricts us to processes with an even number of bosons and therefore we can neglect the odd powers of H_T in Eq. (2.55), resulting in

$$T = H_T(G_0 + G_0 H_T G_0 H_T G_0 + \dots) H_T \equiv H_T G H_T \tag{2.60}$$

where we have defined

$$G = G_0(1 + H_T G_0 H_T G_0 + \dots) = G_0(1 + H_T G_0 H_T G) \tag{2.61}$$

This can be solved for G as

$$G(E) = \frac{1}{E - H_0 - \Sigma(E)} \tag{2.62}$$

with the self-energy $\Sigma(E) = H_T G_0(E) H_T$. It is useful to compare Eq. (2.62) to Eq. (2.36) since both describe retarded Green's functions. However, Eq. (2.36) is a Green's function just for the central device with ω being the resonator energy, whereas Eq. (2.62) applies for the whole system, including the reservoirs, and E is the corresponding total energy.

We now assume the weak-coupling limit so that the real part of Σ, responsible for a shift in the resonance of G, is small enough to be neglected, while the imaginary part is diagonal in the same basis as H_0 and equal to the inverse lifetime of the state. More explicitly, the matrix elements of G are

$$\langle k\sigma | G(E) | k\sigma \rangle = \frac{1}{E - E_{k\sigma} + \frac{i}{2}\Gamma_\sigma} \tag{2.63}$$

Here k and σ refer to the state of the reservoirs and the spin, and $E_{k\sigma}$ is the total energy of the system in state $|k\sigma\rangle$. We have approximated the inverse lifetime of the state $|k\sigma\rangle$ with Γ_σ, the tunneling rate out of spin state σ (to be defined below). From now on we use the notation where $|i\rangle$ and $|f\rangle$ refer only to the reservoir part of the initial and final states, the full system states being given by $|i\sigma\rangle$ and $|f\sigma\rangle$. State with a flipped spin is denoted as $|\bar{\sigma}\rangle = \sigma_x |\sigma\rangle$. Then substituting Eqs. (2.59), (2.60), and (2.63)

in Eq. (2.54) yields

$$\begin{aligned}\Gamma_{i\sigma\to f\sigma} &= 2\pi\left|\sum_k \frac{\langle f\sigma|H_T|k\bar{\sigma}\rangle\langle k\bar{\sigma}|H_T|i\sigma\rangle}{E_i - E_{k\bar{\sigma}} + \frac{i}{2}\Gamma_{\bar{\sigma}}}\right|^2 \delta(E_i - E_f) \\ &= 2\pi c_{j_L}^2 c_{j_R}^2 (N_{j_R,i}+1) N_{j_L,i} \\ &\times \left|\frac{1}{\pm\omega_0 + \omega_{j_L} + \frac{i}{2}\Gamma_{\bar{\sigma}}} + \frac{1}{\pm\omega_0 - \omega_{j_R} + \frac{i}{2}\Gamma_{\bar{\sigma}}}\right|^2 \delta(\omega_{j_L} - \omega_{j_R})\end{aligned} \tag{2.64}$$

where the first term of the sum corresponds to the intermediate state $|k\rangle = a_{j_L}|i\rangle$ and the second term to $|k\rangle = a_{j_R}^\dagger|i\rangle$, and the upper signs apply to the case when the initial state has spin up, that is, the excited state, and lower signs apply to the spin-down ground state.

The rate of heat absorbed from the left bath and emitted to the right bath, conditioned on the spin initially being in state σ, is now given by

$$J_{L\to R}^{(\sigma)} = \sum_{i,j_L,j_R} \omega_{j_L}\Gamma_{i\sigma\to f\sigma} W_i, \tag{2.65}$$

where the sum is over all reservoir initial states (with thermal weights W_i), and over all left and right reservoir oscillators j_L and j_R. An exactly similar formula applies for heat flow in the other direction, with left and right oscillators swapped in Eq. (2.59), and the resulting net heat current is $J^{(\sigma)} = J_{L\to R}^{(\sigma)} - J_{R\to L}^{(\sigma)}$ which can be evaluated as

$$J^{(\sigma)} = \int_0^\infty \frac{d\omega}{2\pi}\,\omega\Gamma_L(\omega)\Gamma_R(\omega)\left|\frac{1}{\omega - \omega_0 \mp \frac{i}{2}\Gamma_{\bar{\sigma}}} - \frac{1}{\omega + \omega_0 \pm \frac{i}{2}\Gamma_{\bar{\sigma}}}\right|^2 \big[n_L(\omega) - n_R(\omega)\big] \tag{2.66}$$

with upper signs for spin up and lower signs for spin down. The reservoir coupling strengths have been defined as $\Gamma_\alpha(\omega) = 2\pi\sum_{j\in\alpha} c_j^2\delta(\omega - \omega_j)$.

We still must find an expression for the total heat current J in terms of the conditional currents $J^{(\sigma)}$, and for that we need the probabilities P_σ to be in spin state σ. It should be noted that the transitions in Eq. (2.64) can be divided into two classes: those where the intermediate state has (roughly) the same energy as the initial state, and those where the energies are different.[1] Using the terminology from electron transport, we call these two processes sequential tunneling and cotunneling, and the current can accordingly be divided into two contributions, $J^{(\sigma)} = J_{\text{seq}}^{(\sigma)} + J_{\text{cot}}^{(\sigma)}$. The intermediate state of a cotunneling process is virtual and does not contribute to P_σ. Therefore the probabilities are determined by sequential processes which can be treated by the first order golden rule of the

[1] This division is non-trivial; see Ref. [29] for a discussion.

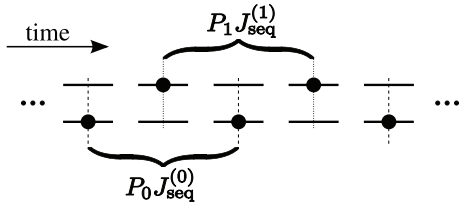

Figure 2.2. Evolution of the spin state due to sequential tunneling events. The current carried by these tunneling events can be calculated in two different ways. On one hand, we can start with the TLS in ground state, and then one current-carrying process flips the state twice, and the next process again starts from the ground state. The average current transported by these processes is $J_{\rm seq} = P_0 J^{(0)}_{\rm seq}$. On the other hand, we can describe the same sequence of events by starting with the spin in the excited state, giving $J_{\rm seq} = P_1 J^{(1)}_{\rm seq}$. Thus the two expressions for sequential current are not additive but alternatives to one another.

previous section. Denoting the spin-down and spin-up states by $\sigma = 0$ and $\sigma = 1$, the golden rule transition rates out of state σ are

$$\begin{aligned} \Gamma_0 &= \Gamma_L(\omega_0) n_L(\omega_0) + \Gamma_R(\omega_0) n_R(\omega_0) \\ \Gamma_1 &= \Gamma_L(\omega_0)[n_L(\omega_0)+1] + \Gamma_R(\omega_0)[n_R(\omega_0)+1] \end{aligned} \tag{2.67}$$

Note that these same rates are used in Eq. (2.66). The steady-state master equation $\dot{P}_0 = -\Gamma_0 P_0 + \Gamma_1 P_1 = 0$, together with $P_0 + P_1 = 1$, can now be solved to

$$P_0 = \frac{\Gamma_1}{\Gamma_0 + \Gamma_1} \tag{2.68}$$

Writing the final expression for the heat current requires some thought since the answer is not what one might initially think. For sequential transport, one current-carrying process consists of two incoherent tunneling events, and if we start with, say, the spin down, then the intermediate state has spin up. But this intermediate state can equally well be seen as the initial state of another sequential process. Because of this overlap, one must be careful to avoid double counting, and as further elucidated in Fig. 2.2, the full sequential current is $J_{\rm seq} = P_0 J^{(0)}_{\rm seq} = P_1 J^{(1)}_{\rm seq}$. On the other hand, cotunneling events are non-overlapping and therefore they contribute additively, $J_{\rm cot} = P_0 J^{(0)}_{\rm cot} + P_1 J^{(1)}_{\rm cot}$. Total heat current through the system, $J = J_{\rm seq} + J_{\rm cot}$, is therefore

$$J = P_0 J^{(0)} + P_1 J^{(1)} - J_{\rm seq} \tag{2.69}$$

We propose that this can be further simplified to

$$J = P_0 J^{(0)} \tag{2.70}$$

This is rigorously true both in the pure sequential tunneling regime where all the three terms in Eq. (2.69) have an equal magnitude, and also in

the low-temperature cotunneling regime where both $J_{\rm seq}$ and P_1 vanish. Simple expressions for J can also be derived in these two limits. At high temperatures, resonant transfer dominates, and this contribution can be extracted by taking the limit $\Gamma_{L,R} \to 0$. Then using Eq. (2.53) on Eq. (2.70) yields [20]

$$J = \omega_0 \frac{\Gamma_L(\omega_0)\Gamma_R(\omega_0)\big[n_L(\omega_0) - n_R(\omega_0)\big]}{\Gamma_L(\omega_0)\big[2n_L(\omega_0)+1\big] + \Gamma_R(\omega_0)\big[2n_R(\omega_0)+1\big]} \tag{2.71}$$

as the high-temperature, sequential tunneling current in the spin–boson model. This result can naturally be also derived just by using the lowest-order approach of Section 2.3.

On the other hand, at low temperatures, $T_{L,R} \ll \omega_0$, the integral in Eq. (2.66) is essentially limited to values of ω much smaller than ω_0, and the ω dependence of the denominator can be neglected, simplifying the integral to

$$J = \int_0^\infty \frac{d\omega}{2\pi} \frac{4\omega\Gamma_L(\omega)\Gamma_R(\omega)}{\omega_0^2}\big[n_L(\omega) - n_R(\omega)\big] \tag{2.72}$$

Crossover between Eq. (2.71) and Eq. (2.72) can be studied numerically from Eq. (2.70).

In contrast to nonequilibrium Green's functions, the theoretical machinery of higher-order golden rule is very simple. The price to be paid is that all different tunneling processes ($N_{L/R}$ bosons absorbed/emitted from left/right) must be separately considered. But this kind of separation does not exist in the real physical system except for some special limits, and this can lead to a complicated entwining of the different contributions, as demonstrated in Fig. 2.2. Going to even higher orders would make the situation quickly unmanageable.

In addition to Publication **I**, the generalized golden rule has also been used in the supplement of Publication **III**.

3. Heat rectification

A transport system is said to be rectifying if current flows preferentially in one direction. Charge rectifiers, or diodes, are vital components in electronics, used, for example, in diode logic gates or AC-to-DC conversion. In comparison, heat diodes, rectifying the flow of thermal energy, have been studied very little so far, the primary reason being that they do not yet have any real-life applications. However, heat diodes, especially mesoscopic ones, are very interesting from a fundamental point of view since they can be used to examine what are the different mechanisms for controlling heat flow in small-scale systems.

To date there are two experiments demonstrating thermal rectification in mesoscopic regime: Chang *et al*. [30] studied phononic heat flow through a mass-loaded nanotube, while Scheibner *et al*. [31] investigated electronic heat transport through a quantum dot at high magnetic fields. Theoretical literature has largely followed the seminal paper by Terraneo *et al*. [32] by concentrating on phonon rectification in one-dimensional atomic chains (see Ref. [24] and references therein). A major problem with 1D diodes is that there does not exist any experimental realization for them, and also their performance is generally not very high. Here we introduce two very different but realistic rectification schemes. The single-electron diode in Section 3.3 is shown to have an especially good performance.

3.1 General considerations

A heat rectifier is defined as a two-reservoir thermal conductor where the *magnitude* of the heat current, and not just the direction, is changed when the reservoir temperatures are swapped. Thus we have two temperatures, a hot T_H and a cold T_C, and we consider two cases: first the left reservoir

is hot ($T_L = T_H$) and the right reservoir is cold ($T_R = T_C$), and then the temperatures are interchanged, $T_L = T_C$ and $T_R = T_H$. The magnitude of the larger heat current in these two cases is J_+, and the smaller one is J_-. We then define *(relative) rectification* as

$$\mathcal{R} = \frac{J_+ - J_-}{J_+} \tag{3.1}$$

Thus a conductor with symmetric heat flow has $\mathcal{R} = 0$ while a maximally asymmetric diode would have $\mathcal{R} = 1$. Of course $\mathcal{R}$ depends on the temperatures $T_{H,C}$, and in particular, in the linear response limit the heat current is proportional to $T_L - T_R$, so that exchanging T_L and T_R only flips the sign. Therefore $\mathcal{R} \to 0$ when the temperature difference is vanishing.

Can either of the devices studied in the previous chapter, a harmonic oscillator or a two-level system, act as a rectifier? Since swapping of the temperatures amounts to the interchange $n_L \leftrightarrow n_R$ in the current formulas, we see that neither a harmonic oscillator [Eq. (2.4)] nor a two-level system at low temperatures [Eq. (2.72)] can rectify heat. However, a two-level system at high temperatures [Eq. (2.71)] has Bose functions nontrivially in the denominator, and if $\Gamma_L \neq \Gamma_R$, heat flow is asymmetric. This spin–boson thermal rectifier, first studied by Segal and Nitzan [20], is one of the simplest systems for asymmetric heat transport, and we will use it to demonstrate some general features of thermal rectification.

The heat transport literature often concentrates on finding devices with large $\mathcal{R}$. However, simply maximizing $\mathcal{R}$ is not a very useful goal, as we now show. Consider Eq. (2.71) with $\Gamma_L < \Gamma_R$, where $\Gamma_\alpha = \Gamma_\alpha(\omega_0)$, and let the Bose functions for the hot and cold reservoir be n_H and n_C, evaluated at ω_0. Then we have $\Gamma_L n_H + \Gamma_R n_C < \Gamma_L n_C + \Gamma_R n_H$, and looking at Eq. (2.71) we see that the larger current J_+ is obtained when the left reservoir is hot and the smaller current J_- is obtained in the opposite case. Then the rectification is

$$\begin{aligned} \mathcal{R} &= 1 - \frac{\Gamma_L(1+2n_H) + \Gamma_R(1+2n_C)}{\Gamma_L(1+2n_C) + \Gamma_R(1+2n_H)} \\ &< 1 - \frac{\Gamma_L T_H + \Gamma_R T_C}{\Gamma_L T_C + \Gamma_R T_H} < 1 - \frac{T_C}{T_H} = \mathcal{R}_{\max} \end{aligned} \tag{3.2}$$

The difference of the Bose functions is maximized in the limit $\omega_0 \ll T_{C,H}$, when we have $n_{C,H} \approx T_{C,H}/\omega_0$. This yields the second expression on the right hand side, which in turn is maximized when $\Gamma_L \ll \Gamma_R$, giving the third expression as the ultimate upper limit for $\mathcal{R}$ in the spin–boson rectifier. This is the *maximum rectification* $\mathcal{R}_{\max}$ for the device at the given temperatures $T_{H,C}$. Because the validity of Eq. (2.71) requires that we

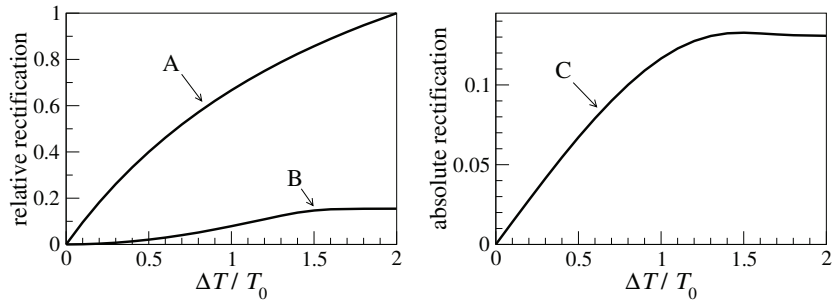

Figure 3.1. Three performance measures for the spin–boson rectifier: (A) Maximum rectification $\mathcal{R}_{\max}$, (B) rectification at maximum current $\mathcal{R}_{J_{\max}}$, and (C) maximum absolute rectification $\Omega_{\max}$. The temperature difference is $\Delta T = T_H - T_C$ and the average temperature is $T_0 = \frac{1}{2}(T_H + T_C)$.

are in the weak-coupling limit with $\Gamma_{L,R}$ smaller than ω_0, the set of conditions for maximal $\mathcal{R}$ can be written as $\Gamma_L \ll \Gamma_R \lesssim \omega_0 \ll T_{C,H}$. But this implies that the heat currents, also the larger current J_+, become vanishingly small compared to the maximum value of Eq. (1.3). Based on the available literature we hypothesize that this is a generic feature for rectifiers: maximizing $\mathcal{R}$ results in a vanishing J_+. This does not mean, however, that $\mathcal{R}_{\max}$ would be a useless measure; quite on the contrary, if we have two devices, one with larger $\mathcal{R}_{\max}$, then this device is also likely to have larger $\mathcal{R}$ at finite current levels.

We clearly also need other ways the characterize heat diodes than $\mathcal{R}_{\max}$, and one obvious strategy is to first maximize the current J_+ and then examine the resulting $\mathcal{R}$. This gives us a new performance measure, *rectification at maximum current*, $\mathcal{R}_{J_{\max}}$. For the spin–boson rectifier we can calculate this quantity for given temperatures $T_{H,C}$ by writing the coupling strengths as $\Gamma_L = (1-\chi)\Gamma$ and $\Gamma_R = (1+\chi)\Gamma$, maximizing J in Eq. (2.71) with respect to χ and ω_0, and then using these values in Eq. (3.2). The results of this numerical calculation are plotted in Fig. 3.1. We see that $\mathcal{R}_{J_{\max}}$ is roughly an order of magnitude smaller than $\mathcal{R}_{\max}$, and in fact, the both diodes presented in the following sections have a vanishing $\mathcal{R}$ under maximum current conditions. Thus $\mathcal{R}_{J_{\max}}$ is also problematic as an efficiency indicator.

What we would like to have is a rectifier with *both* a large $\mathcal{R}$ and a large J_+. As we already noted above, a reasonable way to measure the largeness of current in a device with a single heat conductance channel is to compare it to the current quantum J_Q of Eq. (1.3). Then maximizing both $\mathcal{R}$ and J_+/J_Q is most simply achieved by maximizing their product, and therefore

we introduce another performance metric, the *absolute rectification*

$$\Omega = \mathcal{R}\frac{J_+}{J_Q} = \frac{J_+ - J_-}{J_Q} \tag{3.3}$$

The current asymmetry $J_+ - J_-$ is now compared to the maximal possible current J_Q. If in one direction the heat flow is ballistic, $J_+ = J_Q$, and in the other direction it is fully suppressed, $J_- = 0$, we have $\Omega = 1$. It is difficult to imagine how this kind of device could be constructed, and producing diodes with large Ω is therefore an extremely challenging task. It is an open problem whether there is an upper bound for Ω below the absolute limit of unity. Here we should emphasize the fact that the diodes we are considering must be genuinely two-terminal devices; there cannot be any other energy sources than the two heat baths since otherwise one could have some externally-powered observer who measures the bath temperatures and opens or closes a transmission gate depending on which side is hotter, giving trivially $\Omega \approx 1$.

We can now calculate the *maximum absolute rectification*, $\Omega_{\max}$, in a similar way as $\mathcal{R}_{\max}$ and $\mathcal{R}_{J_{\max}}$ above, and the results are shown in Fig. 3.1. There is one important caveat, however: now the magnitudes of the coupling strengths $\Gamma_{L,R}$ are not cancelled in Eq. (3.3) like they are in Eq. (3.1), and therefore they must be fixed manually. Since Eq. (2.71) is a weak-coupling result, $\Gamma_{L,R}$ must be smaller than ω_0. For Fig. 3.1 we have taken $\Gamma_R = \omega_0$, and then the maximization procedure gives $\Gamma_L \approx 0.25\,\omega_0$. Thus the plot should be considered an upper limit for $\Omega_{\max}$ in the spin–boson diode, and we can conclude that in this system the maximum absolute rectifications are below ten percent.

In summary, we have presented three new performance measures for heat diodes: maximum rectification $\mathcal{R}_{\max}$, rectification at maximum power $\mathcal{R}_{J_{\max}}$, and maximum absolute rectification $\Omega_{\max}$. To the best of our knowledge these quantities have not been considered in the literature before. Interesting open problems include finding the ways these quantities can be maximized and discovering possible relationships between them.

3.2 Weakly nonlinear oscillator

As noted in the previous section, a fully harmonic oscillator is not able to rectify heat flow but the situation is changed if the oscillator is made slightly nonlinear. In Publication **II** we study exactly that kind of system, described by the Hamiltonian (2.7) but with the addition of a quartic

nonlinearity $H'_C = 2\epsilon X^4$ in the central oscillator. We assume that ϵ is small enough that the interaction can be treated at the mean-field level. Since there are six ways two operators can be picked from a set of four, a diagrammatic expansion of the Green's function for the oscillator, $G = \langle X, X\rangle$, shows that in a Hartree approximation we have $X^4 \approx 6\langle X^2\rangle X^2$. We can then write the new H_C also as a harmonic Hamiltonian:

$$H_C = (\frac{1}{2}\omega_0 + 12\epsilon\langle X^2\rangle)X^2 + \frac{1}{2}\omega_0 P^2 = \frac{1}{2}\tilde{\omega}_0(\tilde{X}^2 + \tilde{P}^2) \tag{3.4}$$

The requirement that the rescaled operators obey the commutation relation $[\tilde{X}, \tilde{P}] = i$ results in $\tilde{\omega}_0 = \omega_0\sqrt{1 + 24\epsilon\langle X^2\rangle/\omega_0}$, $\tilde{X} = \sqrt{\tilde{\omega}_0/\omega_0}X$, and $\tilde{P} = \sqrt{\omega_0/\tilde{\omega}_0}P$. The Hartree approximation is assumed to be valid if the change in the oscillator frequency is small, that is, $24\epsilon\langle X^2\rangle \ll \omega_0$.

The heat transport problem can now in principle be solved just like in Section 2.2 though in this case the frequency $\tilde{\omega}_0$ is not a fixed constant but a function of $\langle X^2\rangle$ which can be expressed as

$$\langle X^2\rangle = \langle X(t)X(t)\rangle = i\lim_{t'\to t}\langle X, X\rangle^<(t - t') = \int_{-\infty}^{\infty}\frac{d\omega}{2\pi}i\langle X, X\rangle^<(\omega) \tag{3.5}$$

The lesser Green's function is obtained from the retarded Green's function using Eq. (2.28), which in turn is calculated from Eq. (2.36) with $\tilde{\omega}_0$ replacing ω_0. This yields

$$\langle X^2\rangle = 2\int_{-\infty}^{\infty}\frac{d\omega}{2\pi}\,\frac{\Gamma_L(\omega)n_L(\omega) + \Gamma_R(\omega)n_R(\omega)}{\left|\frac{\omega^2 - \tilde{\omega}_0^2}{\tilde{\omega}_0} + i\Gamma(\omega) - \Lambda(\omega)\right|^2} \tag{3.6}$$

Since $\tilde{\omega}_0$ contains $\langle X^2\rangle$, this integral must be evaluated self-consistently. Heat current is then given by Eq. (2.37) with $\tilde{\omega}_0$ replacing ω_0. Rectification in this system is due to the fact that for a spatially asymmetric device different current directions have a different effective resonance $\tilde{\omega}_0$.

The rectification performance of the nonlinear oscillator can now be examined using the efficiency measures introduced in the previous section. Simplest one is the rectification at maximum current, $\mathcal{R}_{J_{\max}}$: just like at the end of Section 2.1 we can conclude that J is maximized when $\Gamma_L = \Gamma_R \to \infty$, but in this case the transport system is symmetric with no diode behavior, and thus $\mathcal{R}_{J_{\max}} = 0$.

In order to study finite rectification we need a model for the reservoirs. Here we assume that they are RLC circuits with admittances $Y_\alpha(\omega) = R_\alpha^{-1}[1 - iQ_\alpha(\omega/\omega_\alpha - \omega_\alpha/\omega)]^{-1}$, where R_α is the resistance, ω_α the resonance frequency and Q_α the quality factor. Note here one significant advantage of microwave heat transport: for electron or phonon transport tailoring the reservoir density of states is very difficult but in the photonic case

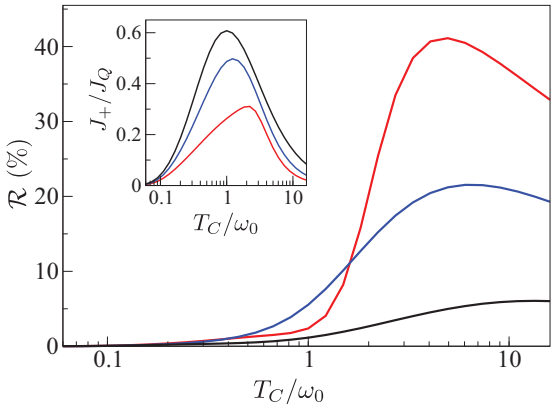

Figure 3.2. Rectification $\mathcal{R}$ and corresponding heat current J_+ in transport through a weakly nonlinear oscillator. Both reservoirs have reactive components with quality factors $Q_L = 0.1$ and $Q_R = 1.0$. The resonance frequency of the right reservoir is $\omega_R = \omega_0$, while the different curves correspond to different values for the left-reservoir frequency: $\omega_L/\omega_0 = 0.1$ (red), 0.2 (blue), and 1.0 (black). The hot temperature is $T_H = 2\,T_C$. Other parameters: $M_L^2\omega_0 L^{-1}R_L^{-1} = 0.1$, $M_R^2\omega_0 L^{-1}R_R^{-1} = 0.8$, $\epsilon/\omega_0 = 0.005$.

it can be readily accomplished by circuit engineering, providing a large amount of flexibility in tuning the device behavior.

Figure 3.2 shows rectification and current for a setup where both reservoirs have a finite quality factor. We see that it is possible to have rectification up to $\mathcal{R} \sim 40\%$ for currents $J_+/J_Q \sim 0.3$. We have not found any operating regime with an essentially higher performance, and thus we conclude that the maximum absolute rectification $\Omega_{\max}$ can be up to about 10% for $T_H/T_C = 2$. The maximum rectification $\mathcal{R}_{\max}$ has not been rigorously studied but our calculations suggest that $\mathcal{R} \gtrsim 50\%$ cannot be achieved with any reasonable parameters values.

We remark that Publication **II** uses a slightly incorrect Hamiltonian for the circuit and therefore the figures are not quantitatively accurate. However, this does not affect the qualitative conclusions of the paper.

Finally we note that the nonlinear oscillator can be experimentally realized with an rf-SQUID loop containing one Josephson junction. As an extra convenience, in this setup the size of the nonlinearity ϵ can be controlled during the experiment with an external magnetic field.

3.3 Single-electron heat diode

In **III** we have studied another type of heat rectifier, depicted in Fig. 3.3. It consists of two small dots between two electronic reservoirs held at differ-

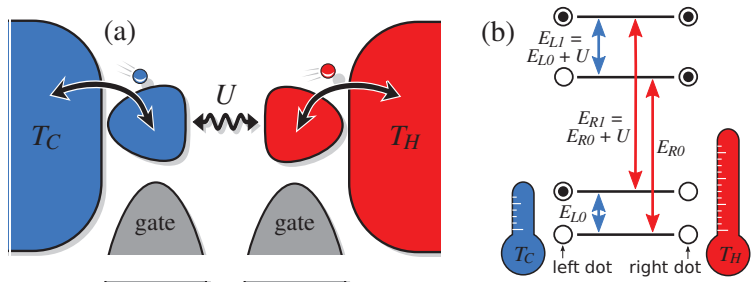

Figure 3.3. (a) Schematic of the single-electron heat diode. Electrons hop in and out of the dots and exchange energy through Coulomb interaction U. (b) Energy-level diagram of the double-dot system.

ent temperatures, and electrons are able to tunnel between the reservoir and the adjoining dot but interdot tunneling is suppressed. Thus there is no electron transport through the device but it is assumed that Coulomb coupling between the dots is strong enough so that *energy* can be transported from one dot to another. Consider now the following cycle: First an electron tunnels into the left dot, then another electron tunnels into the right dot. Because of the Coulomb interaction between the dots, the electron in the left dot forces the second electron to take an extra energy U from the right reservoir. Next the first electron tunnels out of the left dot carrying the interaction energy U with it, and finally the second electron also tunnels back to the right reservoir. Now the electron balance is the same as in the initial state but one energy quantum U has been transported from right to left. This type of heat transport mechanism was first introduced in Ref. [33] but the authors there did not consider rectification. It is important to note that this four-step tunneling cycle (and its time-reverse) is the only way to transport heat between the reservoirs. The diode behavior stems from the fact that one step of this cycle can be efficiently suppressed when the temperature bias is in one direction but all steps are available when the bias is in the other direction. The idea is simply that the energy levels in one dot, say right, are high compared to the other dot. Then if the right reservoir is cold, electrons there do not have enough energy to tunnel into the dot and heat flow is suppressed. If, on the other hand, the right reservoir is hot, all steps of the transport cycle work as described above, carrying heat from right to left.

A minimal model for this type of device is obtained if we assume that the double dot can only be in four different states: empty (energy 0), left dot occupied (energy E_{L0}), right dot occupied (energy E_{R0}), and both dots occupied (energy $E_{L0}+E_{R0}+U$). The spectrum of single-electron states in

the dots is irrelevant for the diode mechanism, and in **III** we consider two explicit examples, a quantum dot with a single sharp level and a metallic dot with a constant density of states. The heat current is then calculated with a master equation and Fermi golden rule, similarly to Section 2.3, and the result for a quantum dot system is

$$J = A^{-1} U \Gamma [n_L(U) - n_R(U)] \tag{3.7}$$

where the prefactor, responsible for the transport asymmetry, is

$$A = \frac{2[1 + n_L(U)][1 + n_R(U)]}{f_{L0}(1 - f_{L1}) f_{R0}(1 - f_{R1})} - 2 \tag{3.8}$$

with $f_{\alpha n} = f_\alpha(E_{\alpha n})$ and $E_{\alpha 1} = E_{\alpha 0} + U$; see Fig. 3.3. Equation (3.7) applies for the case where the two tunnel junctions have equal coupling strengths $\Gamma \equiv \Gamma_L = \Gamma_R$.

Let us first consider the maximum rectification. As was shown in Eq. (3.2), for the spin–boson rectifier the current ratio is limited by $J_+/J_- < T_C/T_H$. For the present systems we see that when the energies E_{L0}, E_{R0} and U are all larger than the temperatures, Eq. (3.7) implies

$$J_+/J_- \approx e^{(T_C^{-1} - T_H^{-1})(E_{R0} - E_{L0})} \tag{3.9}$$

Thus by increasing the large energy E_{R0} it is possible to have arbitrarily large J_+/J_- at any temperatures. In other words, the single-electron heat diode has $\mathcal{R}_{\max} = 1$, independent of temperatures.[1] This shows that the device is a particularly efficient diode. Of course in the limit when $\mathcal{R} \to 1$ the currents become vanishingly small but the important fact is that large rectification is available at finite currents. As an example, the analysis in **III** shows that $\mathcal{R}$ above 0.9 is possible with J_+ in the femtowatt regime.

Next we examine the rectification at maximum current. Numerical calculation shows when J_+ is maximized we have $E_{L0} = E_{R0}$, implying that the system is spatially symmetric, so that there cannot be any rectification. Therefore we conclude that $\mathcal{R}_{J_{\max}} = 0$ at all temperatures. Note, however, that we have assumed symmetric coupling, $\Gamma_L = \Gamma_R$. Relaxing this assumption is likely to yield a finite $\mathcal{R}_{J_{\max}}$.

Another numerical calculation reveals that the maximum absolute rectification, assuming coupling strength $\Gamma = T_0$, gives a result very similar to curve C of Fig. 3.1, with a maximum value of about 0.1. The same warning applies as in the spin–boson case: the value of Γ has been pushed to the upper limits and the actually attainable value of $\Omega_{\max}$ is likely to be up

[1] Naturally in a real physical system E_{R0} cannot be increased indefinitely.

to an order of magnitude lower. Nevertheless, both the spin–boson rectifier and the single-electron diode have quite similar values for $\Omega_{\max}$, even though the latter device is superior in terms of $\mathcal{R}_{\max}$. The reason is that both system operate in the weak-coupling limit while large absolute rectification requires large currents which are not possible in that limit. It is interesting to speculate whether there exists any systems with Ω clearly above 10%. Apparently such systems must have strong couplings and strong interactions since both the weakly coupled, strongly interacting devices of Sections 3.1 and 3.3, and the strongly coupled, weakly interacting device of Section 3.2 perform poorly in terms of Ω.

4. Particle-exchange heat engines

Heat engines can be divided into two main classes, cyclic and particle-exchange heat engines [34]. Thermodynamics textbooks usually present the cyclic type, where heat is carried by a working gas which is alternatingly coupled to the hot and cold reservoirs and work is extracted by an external manipulation of the gas. In contrast, in a particle-exchange device heat is carried by particles propagating between hot and cold reservoirs and work is done by (the same or different) particles being transported up a potential gradient. A thermoelectric power generator is a typical example of the latter type of device.

In this thesis we consider mesoscopic thermoelectric[1] particle-exchange heat engines; a recent review is given in Ref. [35]. Thermoelectric heat engines are particularly well suited for solid-state operation; the periodic coupling between the two heat baths, required by cyclic devices, can be difficult to implement with a non-moving working gas. Furthermore, a particle-exchange device works autonomously, without any time-dependent external control. These kinds of engines are readily incorporated on a microchip, and could be used to recover part of the waste heat produced by electronic components.

4.1 General considerations

A paradigmatic example of a mesoscopic particle-exchange heat engine consists of two electron reservoirs at different temperatures connected by an elastic scatterer. The electric current through the system is given by the Landauer formula of Eq. (1.1), with the electron energy ε replaced by

[1] It is customary to distinguish between *thermoelectric* and *thermionic* devices, depending on whether the electron transport is diffusive or ballistic [35]. For our purposes this distinction is unnecessary.

the electron charge e (remember that we use $k_B = \hbar = e = 1$):

$$I = \int_{-\infty}^{\infty} \frac{d\varepsilon}{2\pi} \mathcal{T}(\varepsilon)[f_L(\varepsilon) - f_R(\varepsilon - V)] \tag{4.1}$$

where a voltage bias V has been applied between the leads. Note that this applies for a single channel, which also means a single spin species, and therefore I should be multiplied by 2 to take into account both spin directions. If an electron with energy ε is removed from the left lead, the entropy of the system is decreased by ε/T_L. Since the elastic scatterer does not change the energy of the electron, it will arrive to the right lead with an energy $\varepsilon - V$ above the chemical potential, corresponding to an entropy increase of $(\varepsilon - V)/T_R$. At the special energy ε^*, obeying

$$\frac{\varepsilon^*}{T_L} = \frac{\varepsilon^* - V}{T_R} \implies \varepsilon^* = \frac{VT_L}{T_L - T_R} \tag{4.2}$$

the entropy of the system remains unchanged, that is, transport is reversible. If we assume that $V > 0$ and $T_L > T_R$, then the heat taken from the hot left reservoir is ε^* and the work done is V, and the energy conversion efficiency from Eq. (4.2) is

$$\eta = \frac{V}{\varepsilon^*} = 1 - \frac{T_R}{T_L} \tag{4.3}$$

which is equal to the Carnot efficiency. If we are able to shape the transmission function so that only electrons at ε^* are allowed to pass through, we have a heat engine with Carnot efficiency. Indeed a quantum dot with a single level at ε^* can approach this ideal limit [36]. There is, however, one major problem: in that case $f_L(\varepsilon^*) - f_R(\varepsilon^* - V) = 0$, implying that current I vanishes. We are now facing a very similar situation as we had in the previous chapter. There we noticed that maximum rectification occurs at vanishing current, and now we see that heat engines have maximum efficiency $\eta_{\max}$ at vanishing output power. Of course we can analogously conclude that devices with a large $\eta_{\max}$ will also have a large η at finite power.

Next we consider the case of maximum *power* and the corresponding *efficiency at maximum power*, $\eta_{P_{\max}}$. In the previous chapter we saw that even high-performance diodes can have $\mathcal{R}_{J_{\max}} = 0$ which makes the relevance of this quantity questionable. In contrast, for heat engines the analogous quantity $\eta_{P_{\max}}$ cannot be vanishing since $\eta = 0$ implies zero power, and for this reason $\eta_{P_{\max}}$ turns out to be a very useful performance indicator which has been studied for decades. Using a particular heat engine model, one can show that $\eta_{P_{\max}}$ has an upper limit of $\eta_{CA} = 1 - \sqrt{T_C/T_H}$.

This result is usually credited to Curzon and Ahlborn [37], although it has been also discovered by others [38, 39]. However, lately it has been shown that the Curzon–Ahlborn result does not apply generally [40] but values of $\eta_{P_{\max}}$ above the purported limit are possible. Despite of this, η_{CA} can act as a convenient yardstick when discussing efficiency at maximum power.

In addition, one could of course introduce yet another efficiency indicator, the product of efficiency η and power P, in analogy to the absolute rectification Ω for heat diodes, but we shall not consider this quantity.

One question still remains. Above we considered efficiency under maximum power conditions. But what is the upper limit for this maximum power in a single-channel device? Although Ref. [41] discusses the conditions for maximum power, an explicit expression has not been derived in the literature. Therefore we present the calculation here. We work under the assumption that Eq. (4.1) is an appropriate starting point. As above, we take $T_L > T_R$, and consider first the unbiased case $V = 0$. The Fermi function difference in Eq. (4.1) shows that at energies $\varepsilon > 0$ the average electron current is from left to right, and in the other direction for $\varepsilon < 0$. If we wish to have maximal current to the right the left-moving part of the transmission spectrum must be suppressed, so that $\mathcal{T}$ must be a step function, $\mathcal{T}(\varepsilon) = \theta(\varepsilon)$. This implies that the maximal single-channel thermoelectric current is

$$I_{\max} = \int_0^\infty \frac{d\varepsilon}{2\pi}[f_L(\varepsilon) - f_R(\varepsilon)] = \frac{\log 2}{2\pi}\Delta T \tag{4.4}$$

where $\Delta T = T_L - T_R$. However, power production is zero since the system is unbiased. At finite bias $V > 0$ the electron flow changes direction at ε^* given by Eq. (4.2), and the corresponding maximum current is

$$I_{\max}(V > 0) = \int_{\varepsilon^*}^\infty \frac{d\varepsilon}{2\pi}[f_L(\varepsilon) - f_R(\varepsilon - V)] = \frac{\log(1 + e^{-\frac{V}{\Delta T}})}{2\pi}\Delta T \tag{4.5}$$

Then the maximum single-channel thermoelectric power is

$$P_{\max} = \max_{V>0} V I_{\max}(V) = \frac{\gamma}{2\pi}(\Delta T)^2 \tag{4.6}$$

where $\gamma \approx 0.3164$ is the maximum value of $x \log(1 + e^{-x})$ which is obtained when $x \equiv V/\Delta T \approx 1.145$.

It should be pointed out that if the intended application of the heat engine is the recovery of waste heat, then the input energy can be considered abundant and available at no cost. In this case efficiency becomes an irrelevant quantity and one should only concentrate on maximizing the output power.

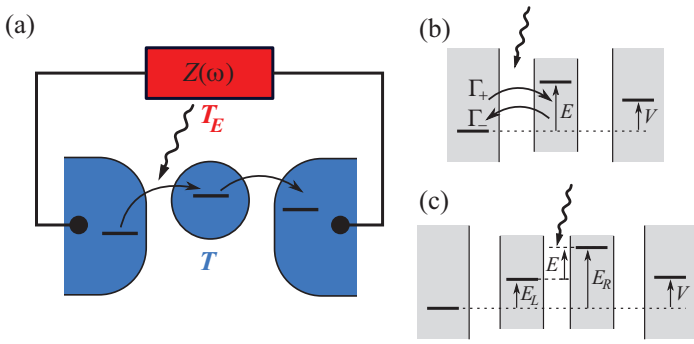

Figure 4.1. (a) Schematic of a single-electron heat engine coupled to an external environment with impedance $Z(\omega)$. Electrons tunneling through the left junction exchange energy with the heat bath, enabling net current against the voltage bias. (b), (c) Energy-level diagrams of junction systems with one or two dots between the leads. One of the junctions, marked with a photon symbol, is coupled to the external bath. The photon-assisted tunneling rates are $\Gamma_{\pm}$.

4.2 Three-reservoir photonic heat engine

In the two-terminal heat engine of the previous section the same electrons were carrying the heat and performing the work. More flexible configurations would be possible if the heat and work flows could be separated to different pathways. This can indeed be achieved in a three-reservoir setup where work is done by transporting electrons from the first to the second reservoir and heat is exchanged between these work electrons and the third reservoir by electromagnetic fields. This type of device was first proposed by Büttiker and coworkers [33, 42]. In their scheme heat is transmitted by local Coulomb interaction just like in the heat diode of Section 3.3. We introduce a more generic setup, depicted in Fig. 4.1, where heat is transported by microwave photons. The device consists of two electron reservoirs which are assumed to be at the same temperature T and a third environment reservoir, modelled by an electromagnetic impedance $Z(\omega)$, at temperature T_E. The electron reservoirs are wired to the impedance, allowing microwaves to propagate through the system. There are also one or two dots between the electron reservoirs, and photon-assisted tunneling through the weakly-coupled junctions can be used to push electrons up against a potential gradient, thereby enabling thermoelectric power generation. We remark that this system bears a close conceptual similarity to a photovoltaic cell where photons from sun enable the transport of electrons against a voltage bias over a p-n junction.

The theoretical method used in the transport calculation is a master equation together with an extension of the Fermi golden rule known as

$P(E)$ theory. That formalism takes in account the coupling to the electromagnetic environment by replacing the energy-conserving $\delta(E_i - E_f)$ in Eq. (2.46) with $P(E_i - E_f)$, the probability density that an energy $E = E_i - E_f$ is emitted ($E > 0$) or absorbed ($E < 0$) by the tunneling electron. Otherwise the calculation proceeds essentially as outlined in Section 2.3. Full account of $P(E)$ theory is given in Ref. [43].

Our basic heat engine idea does not depend on the energy spectrum of the dots, and we exemplify the mechanism both with single-level quantum dots and with metallic dots having constant densities of states. We consider the cases of one or two dots between the reservoirs, which can also be considered as arrays of two or three tunnel junctions in series. We concentrate on the simplest model where intradot Coulomb interaction is large enough so that each dot can only be empty or singly occupied. Then the analysis in **IV** shows that the thermoelectric current is maximized if one of the junctions has weaker tunnel coupling but stronger environment coupling than the other junctions. This requirement is physically well motivated since junctions with weaker tunneling generally have smaller a capacitance C, implying a larger electromagnetic coupling through the charging energy $e^2/2C$. When the environment-coupled junction dominates the dynamics, charge current through the system can be written with very compact formula:

$$I = f(V - E)\Gamma_+ - f(E - V)\Gamma_- \tag{4.7}$$

where $f(\varepsilon)$ is the Fermi function for the electron system, V is the bias, $\Gamma_{+/-}$ are the photon-assisted tunneling rates to the right/left through the environment-coupled junction, and E is the level difference over the junction; see also Fig. 4.1. To be more precise, we now have three possible junction types: (i) junction between a metallic lead and a metallic dot, where E is the difference of the Fermi levels; (ii) junction between a metal and a quantum dot, where E is the difference between the metal Fermi level and the single level of the dot; and (iii) junction between two quantum dots, where E is the dot level difference. Coulomb charging energies of the dots are also included in E.

We use a convention where $I > 0$ means current from left to right, $V > 0$ means that the right lead has a higher potential and $E > 0$ means that the right side of the junction is at a higher energy. We fix $E > 0$ and consider first an unbiased system ($V = 0$). If the environment is hotter than the electron system, then $I > 0$ because electrons are, on the average, absorbing heat from the hot bath by going up the level difference E.

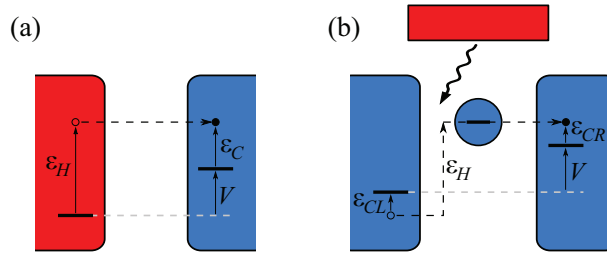

Figure 4.2. Comparison of transport processes in (a) two-reservoir and (b) three-reservoir heat engines. The electron is taken from the left lead to the right and work V is produced. Heat extracted from the hot bath is ε_H and heat deposited in the cold bath is ε_C. In the three-reservoir case ε_H is absorbed from the environment and $\varepsilon_C = \varepsilon_{CL} + \varepsilon_{CR}$ is divided between between the two leads. Energy conservation implies $\varepsilon_H = V + \varepsilon_C$. In (b) the central element is a single-level quantum dot.

The opposite conclusion applies for a cold environment and hot electrons. Power can be now generated by applying a finite bias. The direction of the bias must be chosen so that the thermally driven electrons are pushed up against the voltage, that is, if the zero-bias current is $I > 0$, bias must be $V > 0$. When the magnitude of the voltage is large enough, the current vanishes and then changes direction. From Eq. (4.7) this stopping voltage is

$$V_0 = E - T \log \frac{\Gamma_-}{\Gamma_+} \tag{4.8}$$

The device operates as a heat engine for voltages between zero and V_0.

We now compare the energy transport processes in the two and three-reservoir heat engines; see Fig. 4.2. For the two-reservoir system we assume that the left lead is hot, for the three-reservoir case the environment is hot. When an electron is transported from left to right, heat ε_H is extracted from the hot bath, work V is performed against the voltage bias, and the remaining energy is expelled as heat ε_C into the cold bath. In the three-reservoir case the whole electron transport system constitutes the cold bath and in general ε_C gets divided between the different parts. It is important to notice that when the central element in the three-reservoir device is a single-level quantum dot there is a one-to-one mapping between the processes in the two devices. This is most easily demonstrated by an example. Let us add a single-level quantum dot between the two reservoirs in Fig. 4.2(a), so that the dot level is an energy E above the left lead Fermi level. Then transport can only take place with $\varepsilon_H = E$. But for the three-reservoir case the same result can be obtained by adding another quantum dot between the left reservoir and the first dot, so that the level of the new dot is an energy E below the other dot's level. Also in

this case we have transport only with $\varepsilon_H = E$. Therefore it is possible to filter the energy spectrum exactly in the same way in both cases, and in particular, choosing $E = \varepsilon^*$ from Eq. (4.2) yields Carnot efficiency for both device types.

To investigate the generated power one must consider also the tunneling rates, not just the sizes of the energy packets. In this case the two and three-reservoir engines are very different. The best way to facilitate the comparison is to write the current as an integral over the energy ε_H taken from the hot bath. For the two-reservoir case we have trivially from Eq. (4.1)

$$I = \int_{-\infty}^{\infty} \frac{d\varepsilon_H}{2\pi} \mathcal{T}(\varepsilon_H)[f_H(\varepsilon_H) - f_C(\varepsilon_H - V)] \tag{4.9}$$

where $f_{H,C}$ are Fermi functions at the hot and cold temperatures $T_{H,C}$. Then writing out Eq. (4.7) gives for the three-reservoir case

$$I = \Gamma \int_{-\infty}^{\infty} d\varepsilon_H f_C(V - E) f_C(E - \varepsilon_H) P(\varepsilon_H)[e^{-\frac{\varepsilon_H}{T_H}} - e^{-\frac{\varepsilon_H - V}{T_C}}] \tag{4.10}$$

where the environment spectrum $P(\varepsilon_H)$ also depends on T_H. We see that the functional dependence of I on the energies ε_H and V and the temperatures $T_{H,C}$ is clearly different in these two cases, so that there is no simple correspondence between the systems when power generation is considered. More detailed investigation requires some explicit form for the environment spectrum. In **IV** we have studied an impedance $Z(\omega)$ describing either an ohmic resistor or a harmonic oscillator. Here we summarize the results very briefly by noting that the maximum achievable power is at least an order of magnitude smaller than the limit given in Eq. (4.6). This result is quite expected since the three-reservoir device is based on Coulomb blockade and it is therefore weakly coupled. One might consider boosting the electron transport by increasing the tunnel coupling, but this will usually decrease the environment coupling which is necessary for the thermoelectric effect. Whether it is possible to overcome this obstacle is an interesting question for future work.

5. Conclusions

In this Thesis we have investigated heat transport in interacting mesoscopic devices. In the systems under study heat flow is determined by the dynamics of electrons or photons or both, and we have treated them with theoretical methods based on perturbation theory: master equations with Fermi golden rule for weakly coupled systems, and nonequilibrium Green's functions for systems with arbitrary couplings. Transport through a nonequilibrium spin–boson model has been examined in detail.

Two new types of heat rectifiers were introduced, namely a nonlinear electromagnetic oscillator and a single-electron heat diode. The oscillator system is able to produce large currents but rectification performance is not very high. In the single-electron diode currents are limited by the requirement to operate in the weak-coupling limit, but very high rectification is available. It is an open problem how to produce both large currents and large rectification.

We also propose a new class of particle-exchange heat engines where work is done by electrons transported between two reservoirs but heat is exchanged between the transport system and a third reservoir by microwave photons. Heat and charge flows are therefore separated, offering much greater flexibility than usual thermoelectrics; for example, the two heat baths can be separated by a large distance. We have shown that the structure of the energy transport processes is similar to the more usual two-reservoir devices, and therefore same efficiencies, up to the Carnot efficiency, are available. However, since the scheme is based on Coulomb blockade, the generated power is limited to weak-coupling values. It is an open problem how to produce a three-reservoir heat engine with large maximum power.

Bibliography

[1] F. Giazotto, T. T. Heikkilä, A. Luukanen, A. M. Savin, and J. P. Pekola, Rev. Mod. Phys. **78**, 217 (2006).

[2] D. R. Schmidt, R. J. Schoelkopf, and A. N. Cleland, Phys. Rev. Lett. **93**, 045901 (2004).

[3] B. J. van Wees, H. van Houten, C. W. J. Beenakker, J. G. Williamson, L. P. Kouwenhoven, D. van der Marel, and C. T. Foxon, Phys. Rev. Lett. **60**, 848 (1988).

[4] D. A. Wharam, T. J. Thornton, R. Newbury, M. Pepper, H. Ahmed, J. E. F. Frost, D. G. Hasko, D. C. Peacock, D. A. Ritchie, and G. A. C. Jones, J. Phys. C **21**, L209 (1988).

[5] R. Landauer, IBM J. Res. Dev. **1**, 223 (1957).

[6] S. Datta, *Electronic Transport in Mesoscopic Systems* (Cambridge University Press, Cambridge, 1997).

[7] L. G. C. Rego and G. Kirczenow, Phys. Rev. Lett. **81**, 232 (1998).

[8] J. B. Pendry, J. Phys. A: Math. Gen. **16**, 2161 (1983).

[9] L. G. C. Rego and G. Kirczenow, Phys. Rev. B **59**, 13080 (1999).

[10] O. Chiatti, J. T. Nicholls, Y. Y. Proskuryakov, N. Lumpkin, I. Farrer, and D. A. Ritchie, Phys. Rev. Lett. **97**, 056601 (2006).

[11] K. Schwab, E. A. Henriksen, J. M. Worlock, and M. L. Roukes, Nature (London) **404**, 974 (2000).

[12] M. Meschke, W. Guichard, and J. P. Pekola, Nature **444**, 187 (2006).

[13] A. V. Timofeev, M. Helle, M. Meschke, M. Möttönen, and J. P. Pekola, Phys. Rev. Lett. **102**, 200801 (2009).

[14] H. B. Callen and T. A. Welton, Phys. Rev. **83**, 34 (1951).

[15] L. M. A. Pascal, H. Courtois, and F. W. J. Hekking, Phys. Rev. B **83**, 125113 (2011).

[16] H. Haug and A.-P. Jauho, *Quantum Kinetics in Transport and Optics of Semiconductors* (Springer-Verlag, Berlin, 2008).

[17] T. Ojanen and A.-P Jauho, Phys. Rev. Lett. **100**, 155902 (2008).

[18] J.-S. Wang, J. Wang, and J.T. Lü, Eur. Phys. J. B **62**, 381 (2008).

[19] H. Bruus and K. Flensberg, *Many-Body Quantum Theory in Condensed Matter Physics* (Oxfo rd University Press, Oxford, 2004).

[20] D. Segal and A. Nitzan, Phys. Rev. Lett. **94**, 034301 (2005).

[21] D. Segal, Phys. Rev. B **73**, 205415 (2006).

[22] D. Segal and A. Nitzan, Phys. Rev. E **73**, 026109 (2006).

[23] D. Segal, Phys. Rev. Lett. **101**, 260601 (2008); J. Chem. Phys. **130**, 134510 (2009).

[24] L.-A. Wu and D. Segal, Phys. Rev. Lett. **102**, 095503 (2009); L.-A. Wu, C. X. Yu, and D. Segal, Phys. Rev. E **80**, 041103 (2009).

[25] L.-A. Wu and D. Segal, Phys. Rev. E **83**, 051114 (2011).

[26] C. X. Yu, L.-A. Wu, and D. Segal, J. Chem. Phys. **135**, 234508 (2011).

[27] K. A. Velizhanin, H. Wang, and M. Thoss, Chem. Phys. Lett. **460**, 325 (2008).

[28] K. A. Velizhanin, M. Thoss, and H. Wang, J. Chem. Phys. **133**, 084503 (2010).

[29] Yu. V. Nazarov and Ya. M. Blanter, *Quantum Transport* (Cambridge University Press, Cambridge, 2009).

[30] C. W. Chang, D. Okawa, A. Majumdar and A. Zettl, Science **314**, 1121 (2006).

[31] R. Scheibner, M. König, D. Reuter, A. D. Wieck, C. Gould, H. Buhmann, and L. W. Molenkamp, New J. Phys. **10**, 083016 (2008).

[32] M. Terraneo, M. Peyrard and G. Casati, Phys. Rev. Lett. **88**, 094302 (2002).

[33] R. Sánchez and M. Büttiker, Phys. Rev. B **83**, 085428 (2011).

[34] T. E. Humphrey and H. Linke, Physica E **29**, 390 (2005).

[35] A. Shakouri, Annu. Rev. Mater. Res. **41**, 399 (2011).

[36] T. E. Humphrey, R. Newbury, R. P. Taylor, and H. Linke, Phys. Rev. Lett. **89**, 116801 (2002).

[37] F. Curzon and B. Ahlborn, Am. J. Phys. **43**, 22 (1975).

[38] I. I. Novikov, J. Nuclear Energy II **7**, 125 (1958) [Atomnaya Energiya **3**, 409 (1957)].

[39] P. Chambadal, *Les Centrales Nucléaires* (Armand Colin, 1957).

[40] M. Esposito, K. Lindenberg, and C. Van den Broeck, Phys. Rev. Lett. **102**, 130602 (2009).

[41] T. E. Humphrey and H. Linke, J. Phys. D **38**, 2051 (2005).

[42] B. Sothmann, R. Sánchez, A. N. Jordan, and M. Büttiker, arXiv:1201.2796.

[43] G. L. Ingold and Yu.V. Nazarov, in *Single Charge Tunneling*, edited by H. Grabert and M. H. Devoret, NATO ASI Series B Vol. 294 (Plenum Press, New York, 1992), pp. 21–107.

Errata

Publication II

Equation (10) should read

$$\Sigma^r(\omega) = -\frac{i\tilde{I}_0^2\omega^3}{\hbar\omega_0^2}\Big[M_L^2 Y_L(\omega) + M_R^2 Y_R(\omega)\Big],$$

and Eq. (11) should read

$$\Sigma^<(\omega) = -\frac{2i\tilde{I}_0^2\omega^3}{\hbar\omega_0^2}\Big[M_L^2 \mathrm{Re}[Y_L(\omega)] n_L(\omega) + M_R^2 \mathrm{Re}[Y_R(\omega)] n_R(\omega)\Big],$$

which imply that the function $F(\omega)$ in Eq. (13) is

$$F(\omega) = \hbar\omega_0(\omega^2 - \omega_0^2 - 12\omega_0\epsilon\Phi)/(2I_0^2\omega^2).$$

Figures with $\mathcal{R}$ and J_+ are therefore quantitatively inaccurate but the qualitative conclusions are unaffected.

There is also a typographical error in the second column of page 3: the single-channel maximum heat current is $J_{\max} = \frac{\pi k_B^2}{12\hbar}(T_{\mathrm{high}}^2 - T_{\mathrm{low}}^2)$.

Aalto-DD 96/2012

ISBN 978-952-60-4714-0
ISBN 978-952-60-4715-7 (pdf)
ISSN-L 1799-4934
ISSN 1799-4934
ISSN 1799-4942 (pdf)

Aalto University
School of Science
Department of Applied Physics
www.aalto.fi

BUSINESS +
ECONOMY

ART +
DESIGN +
ARCHITECTURE

SCIENCE +
TECHNOLOGY

CROSSOVER

**DOCTORAL
DISSERTATIONS**